

**STUDIES ON PARAMAGNETIC AND
REDOX PROPERTIES OF SOME
METALLOPORPHYRINS**

ABSTRACT

*A thesis submitted in fulfillment of the requirements for
the degree of Doctor of Philosophy*

By

A. Murugan

DEPARTMENT OF CHEMISTRY

SCHOOL OF PHYSICAL SCIENCES

NORTH EASTERN HILL UNIVERSITY

SHILLONG - 793 022

April - 2008



NEW LIBRARY
Acc. No. 104334
Ac. by B. Banson
Iss. by 7/8/12
Lending by
Know by

DS
547.593
MUR.1
;

ABSTRACT

Metalloporphyrins broadly falls under two catalogs, viz., naturally occurring and synthetically modified metalloporphyrins/porphyrins. Synthetically modified porphyrins and metalloporphyrins are interesting to study because they serve as biological model systems. On the other hand they also exhibit properties permit than to use in the field of medicines(photodynamic therapy of cancer) and also possibilities of using then in the field of material sciences(semi-conductors etc). Obviously, porphyrin chemistry expands and progresses. This thesis embodies the physico-chemical studies of some vanadyl porphyrins which are not reported in the literature so far. It also incorporated a small chapter on the electrochemistry of some manganese, cadmium and copper porphyrins which are not reported in the literature.

This thesis consists of five chapters.

Chapter 1 presents a brief review of the EPR and Cyclic voltammetric studies of some vanadyl porphyrins.

Chapter 2 describes different experimental techniques and measurements used in the course of investigation.

Chapter 3 presents cyclic voltammetric studies of some vanadyl porphyrins.

Chapter 4 deal with cyclic voltammetric studies of some manganese, cadmium and Copper porphyrins.

Chapter 5 describes EPR of some substituted vanadyl meso-tetraphenyl porphyrins oxidized with SbCl_5

Chapter 1 presents a brief review on vanadyl porphyrins of substituted TPP systems mainly focusing on the electron paramagnetic resonance (EPR) and Cyclic voltammetric (CV) Studies.

Chapter 2 deals with the general experimental techniques and the synthesis of porphyrin and metalloporphyrins, purification of solvents and other reagents used in cyclic voltammetric and ESR studies. $[\text{T}(2,5\text{-(OCH}_3)_2\text{)PP}]$, $[\text{T}(o\text{-NO}_2)\text{PP}]$, $[\text{T}(p\text{-OH)PP}]$, TPyP and its vanadyl complexes were prepared according to methods described in literature. The crude compound was purified by silica gel column chromatography using dichloromethane. It was conformed by UV spectrophotometer.. Vanadyl, manganese, copper and cadmium porphyrins were prepared according to the method as described in the literature. The crude compound was purified by silica gel column chromatography using dichloromethane. It was conformed by UV spectrophotometer

Chapter 3 presents cyclic voltammetric studies of some vanadyl porphyrins. Dichloromethane and tetra-n-butyl ammonium

perchlorate were used as solvent and supporting electrolyte respectively. Cyclic voltammetric studies were done on vanadyl porphyrins viz [VO[T(2,5-(OCH₃)₂)PP], VO[T(o-NO₂)PP], VO[T(p-OH)PP], and VO[TpyP]. All the CV measurements were done with 10⁻³ M solutions of the metalloporphyrins.

The voltammogram of [VO[T(2,5-(OCH₃)₂)PP] indicate the oxidation potentials are slightly higher than that of the VOTPP by about 0.085V and 0.054V respectively. The reason for lowering the oxidation potentials in the case of [VO[T(2,5-(OCH₃)₂)PP] may be because of symmetrical substitution of the phenyl ring which puts it more or less in the similar geometry to that of VOTPP. Although the shifts in the potential either way are small they are quite uniform. This gives us some thoughts to suggest that there are some changes in the geometry of the molecule on substitution which affect the energy levels (HOMO) of the molecule hence shifts in the redox potentials occurs. In fact the voltammogram is of successive one electron transfer of the porphyrin ligand and are reversible. The voltammogram of the VO[T(p-OH)PP] is not a straight forward successive one electron transfer process. The first oxidation potential and its corresponding reduction potential are lower than that of VOTPP, while the second oxidation shows very strong oxidation peak current. The peak current corresponds to more than

one electron transfer. Clearly, the second oxidation involved a process which is irreversible along with the reversible process. This could be due to the formation of secondary oxidation states involving the phenolic groups. leading to oxidative electro polymerizations. On subsequent scanning the peak current decreases leading to film formation at the electrode surface. The electron donating group (-OH) increases the electron density of the macrocycle making the removal of electron easier. Thus, the oxidation potential decreases. The redox process of VO[T(*o*-NO₂)PP], is in line with the redox process of [VO[T(2,5-(OCH₃)₂)PP] . The first oxidation potential is lower than that of VOTPP. This could be due to the structure factor,. The oxidation potentials of VOTpyP are observed to be lower than that of the VOTPP. It is most likely that the lower in oxidation potentials is due to metal d_{xy} porphyrin orbital (a_{2u}) interaction in ruffle distortion and metal dx²-y² porphyrin orbital (a_{2u}) in saddle distortion.

Chapter 4 deal with cyclic voltammetric studies of some manganese, cadmium and Copper porphyrins. Mn[T(2,5-(OCH₃)₂)PP], Mn[T(*o*-NO₂)PP], Mn[T(*p*-OH)PP], Mn[TpyP]. Cd[T(2,5-(OCH₃)₂)PP], Cd[T(*o*-NO₂)PP], Cu[T(2,5-(OCH₃)₂)PP] and Cu[T(*o*-NO₂)PP] All the CV measurements were done with 10⁻³ M solutions of the metalloporphyrins. Manganese porphyrin show

Mn(II) to Mn(III) oxidations. Except Mn[T(*p*-OH)PP] other three manganese porphyrins exhibit two ligand oxidations. These oxidation potentials are slightly on the lower side. This may be due to structural changes. Mn[T(*p*-OH)PP] shows polymerization at electrode surface.

In the case Cd and Cu porphyrins, two ligand redox potentials are observed. The redox process involved successive one electron transfer and are reversible. Oxidation potentials are observed to be slightly lower than that of these respective to TPP complexes. This is reversibility due to the distortions in the structure. Further, effect of electron donating and electron withdrawing groups are also reflected on the redox potentials.

Chapter 5 describes EPR of some substituted vanadyl meso-tetraphenyl porphyrins oxidized with SbCl₅. Except for the VO[T(*p*-OH)PP] other three vanadyl porphyrins undergo oxidation with SbCl₅ generating radical cations in the same process to that of the oxidation of VOTPP. In case of VO[T(*o*-NO₂)PP]. It clearly undergoes oxidation quite similar to that of the oxidation of VOTPP. VO[T(*p*-OH)PP] polymerizes an oxidation. Other, Vanadyl porphyrins form triplet state which are observable at room temperature at higher modulation. Pre-oxidized complexes are also observable at room temperature.

NEHU LIBRARY
Acc. No. 104334
Acc. by. B. Ramon
Date. 17/8/12
Class by. _____
Sub - Heading by. _____
Enter by. _____

**STUDIES ON PARAMAGNETIC AND REDOX
PROPERTIES OF SOME METALLOPORPHYRINS**

*Thesis submitted in fulfillment of the
requirement for the degree of
Doctor of Philosophy*

By

A. Murugan

**DEPARTMENT OF CHEMISTRY
SCHOOL OF PHYSICAL SCIENCES
NORTH EASTERN HILL UNIVERSITY
SHILLONG - 793 022**

April 2008



NEHU LIBRARY

Acc. No. 104334

Acc. by B. Bamon

D. no. 17/8/12

Class by. _____

Sub - Heading by. _____

Enter by. 2/11

DS
547.593
MUR;1
)

Declaration

North-Eastern Hill University

Shillong-793 022

April 2008

I, **A.Murugan**, hereby declare that the subject matter of this thesis is the record of work done by me, that the contents of this thesis did not form basis of the award of any previous degree to me or to the best of my knowledge to anybody else, and that the thesis has not been submitted by me for research degree in any other University/Institute.

This is being submitted to the North-Eastern Hill University for the **Ph.D Degree in Chemistry**.



(A. Murugan)

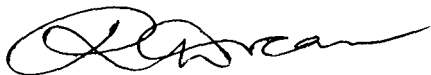
CANDIDATE



(Dr. Aka Lemtur)

SUPERVISOR

Reader
Department of Chemistry
North-Eastern Hill University
Shillong- 793022.



(Prof. R. H. Duncan Lyngdoh)

HEAD

DEPARTMENT OF CHEMISTRY,

NORTH-EASTERN HILL UNIVERSITY

SHILLONG.

Head

Department of Chemistry
North-Eastern Hill University
Shillong- 793022.

Dr. A. Lemtur
Department of Chemistry
North Eastern Hill University
Shillong 793022



email: lemtur1@rediffmail.com
tel. no. 0364 272 2618
fax no: 0364 2550076

CERTIFICATE

This is to certify that the thesis entitled "Studies on paramagnetic and redox properties of some metalloporphyrins" is based on the original work done by A. Murugan, under my supervision in the Department of Chemistry, School of Physical Sciences, North Eastern Hill University, Shillong Meghalaya. This work has not previously formed the basis for the award of any degree, diploma, associateship, fellowship or any other similar title and that it represents entirely an independent work on the part of the candidate.

Prof. R. H. Duncan Lyngdoh

Head

Department of Chemistry

Dr. AKA Lemtur

Supervisor

Place: Shillong

Date: 29.04.08

Acknowledgments

I am extremely grateful and deeply indebted to my supervisor **Dr. Aka Lemtur**, Reader, Department of Chemistry, NEHU, Shillong for his stimulating guidance, constant encouragement and untiring help throughout the course of the study.

I would like to thank the Head, Department of Chemistry, **Prof. R. H. Duncan Lyngdoh**, NEHU, Shillong for all the help rendered to me.

It is with great pleasure; I record my gratitude to **Prof. K. Ismail**, Dean, School of Physical Science, NEHU, and Shillong for his constant help and encouragement throughout the course of this work.

I have immense pleasure in recording my profound sense of gratitude to **Prof. R. K. Poddar**, Department of Chemistry, NEHU, Shillong for his constructive suggestions during every stage of my research work. My thanks go to the Department of Chemistry, NEHU, Shillong, for all the facilities available and to all the faculty members for their gracious encouragement.

I am also thankful to **Prof. N. Venugopal**, Department of Botany, NEHU, and **Mr. Isias**, Teacher, St'Mary Hr.Sec.School, Shillong for their inspiration and untiring help during my stay at Shillong.

I thank my senior and labmate **Dr. A. Tomba Singh**, **Dr(Mrs) Cornelia Mr. Donborlang**, **Mrs. Aicydalyne Snaitang** for their help and moral *Support*.

I owe my sincere thanks to **Prof. J. Subramanian**, NMR Section, CLRI, Chennai, **Prof. P. Sambasiva Rao**, **Mr. B. Natarajan**, Department of Chemistry, Pondicheery University, Pondicheery, **Dr. V. Manivannan**, Department of Chemistry, IITGuwahati and **Mr. Sivaramakrishnan**, SAIF, IIT Madras, Chennai for their help in the EPR measurement. I am also thankful to **Prof. P. R. Athappan** and **Mr. Prabakaran**, Department of Inorganic Chemistry, Madurai Kamaraj University, Madurai for their help in the CV measurements.

I express my sincere thanks to the **Prof. O. K. Medhi**, Department of Chemistry, Gauwahati University, Guwahati for his keen interest in my work.

I would like to express my thanks to **Mrs. Florence** for recording the UV spectra. My sincere gratitude goes to **Mr. Thomas** and other office staff for their help, rendered to me during the course of my Ph.D work.

I owe my sincere thanks to **Dr. Kiranmay Sarma**, Faculty USEM Guru Gobind Sing Indraprastha University, Kashmere Gate, New Nelhi, **Dr. Om Prakash Tripathi**, Lecturer in Forsty Department, NERST, Arunachal Pradesh, **Dr. Krishna Upadya**, Faculty in NEHU, Shillong, **Dr. Bidyadhar Das** for their support, help and inspiration.

Thanks are also due to my friends, **Dr. S. Jeeva**, **Dr. A. Murugesan**, **Dr. Senthikumar**, **Dr. P. Sudhakar**, **Mr. P. RajKumar**, **Dr. A. Shankaran**, **Mr. Kathirvel**, **Mr. K. Dharmaraj**, **Mr. Mithun Chakrabarty**, **Miss. Snigdha Chanda**, **Miss. Juthika Das**, **Miss. Dipannita Das**, **Mr. Johar Dey**, **Mr. Joseph Jeremiah**, **Mr. Haans J.Freddy**, **Mr. Allen J.Freddy**, **Mr. A. Venkateswara Rao**, **Mr. K. Thirumala Prasad** and **Mr. N. Ambikapathy** who have helped in various aspects during the course of the my research work express my sincere gratitude to my beloved Parents and brothers for their co-operation, encouragement and inspiration for completing this research work successfully.

"My help cometh from the Lord which made heaven and earth". Lastly I express my gratitude to God Almighty without whom I would have not been able to complete this research work. I also dedicate this work to Him.

A. Murugan

Contents

	Page No
List of Tables	(i)
List of Figures	(ii)
Preface	1
Introduction	3
References	4
Chapter 1. A brief review of the ESR and cyclic voltammetric studies of some vanadyl porphyrins	7
References	11
Chapter 2. Experimental Section	
2.1. Introduction	13
2.2. Solvents	13
2.3. Oxidizing agent	14
2.4. Reagents and supporting electrolytes	14
2.5. Synthesis of porphyrins	15
2.6. Synthesis of metalloporphyrins	18
2.7. Instrumentation	21
References	23
Chapter 3. Cyclic voltammetric studies of some Vanadyl metalloporphyrins	
3.1. Introduction	24
3.2. Principle of cyclic voltammetry	30
3.3. Experimental details	34
3.4. Results and discussion	34
3.5. Conclusion	40
References	46

Chapter 4. Cyclic voltammetric studies of some manganese, cadmium and copper porphyrins

4.1. Introduction	48
4.2. Results of manganese porphyrins	48
4.3. Discussion of manganese porphyrins	50
4.4. Conclusion of manganese porphyrins	51
4.5. Results of cadmium and copper porphyrins	52
4.6. Discussions of cadmium and copper porphyrins	53
4.7. Conclusion of cadmium and copper porphyrins	53
References	69

Chapter 5. ESR of some substituted vanadyl meso tetraphenylporphyrins oxidized with SbCl_5

5.1. Introduction	71
5.2. Some basic principles of ESR	72
5.2.1. Resonance condition, g-value and symmetry	72
5.2.3. Zerofield splitting and fine structure	75
5.3. Hyperfine interaction	77
5.4. Line shape and relaxation	78
5.5. Spin Hamiltonian	80
5.6. Metalloporphyrins with paramagnetic metal atom unpaired electron on the ligand	81
5.7. ESR of some substituted vanadyl mesotetrapheny porphyrins oxidized with SbCl_5	83
5.7.1. Results	83
5.7.2. Discussion	84
5.7.3. Conclusion	85
References	96

LIST OF TABLES

	Page No.
Table:3.1.Cyclic voltammetric data for vanadyl porphyrins at room Temperature	41
Table:4.1. Cyclic voltammetric data for manganese porphyrins at room temperature	55
Table:4.2.Cyclic voltammetric data for Cadmium and Copper porphyrins at room temperature	64
Table.5.1: ESR spectrum of Vanadyl porphyrins at room temperature	86

LIST OF FIGURES

	Page No
Figure.3.1.1a. Structure of free porphyrin and metalloporphyrin	25
Figure.3.1.1b. Structure of free porphyrin and metalloporphyrin	26
Figure.3.1.2. HOMO representation for metalloporphyrins	28
Figure.3.2.1. Electrochemical cell for quality cyclic voltammetry experiment.	31
Figure.3.2.2. Triangular wave	32
Figure.3.4.1. Cyclic voltammogram of VO[T(2,5-(OCH ₃) ₂)PP] in CH ₂ Cl ₂ Containing 0.1M TBAP at room temperature	42
Figure.3.4.2. Cyclic voltammogram of VO[T(<i>p</i> -OH)PP] in CH ₂ Cl ₂ Containing 0.1M TBAP at room temperature	43
Figure.3.4.3. Cyclic voltammogram of VO[T(<i>o</i> -NO ₂)PP] in CH ₂ Cl ₂ Containing 0.1M TBAP at room temperature	44
Figure.3.4.4. Cyclic voltammogram of VO[T <i>py</i> P] in CH ₂ Cl ₂ Containing 0.1M TBAP at room temperature	45
Figure.4.2.1. Cyclic voltammogram of Mn[T(2,5-(OCH ₃) ₂)PP] in CH ₂ Cl ₂ Containing 0.1M TBAP at room temperature	56
Figure.4.2.2. Cyclic voltammogram of Mn[T(<i>p</i> -OH)PP] in CH ₂ Cl ₂ Containing 0.1M TBAP at room temperature	57
Figure.4.2.3. Cyclic voltammogram of Mn[T(<i>o</i> -NO ₂)PP] in CH ₂ Cl ₂ Containing 0.1M TBAP at room temperature	58
Figure.4.2.4. Cyclic voltammogram of Mn[T <i>py</i> P] in CH ₂ Cl ₂ Containing 0.1M TBAP at room temperature	59
Figure.4.3.1. UV-visible absorption spectrum of Mn[T(2,5-(OCH ₃) ₂)PP] in CH ₂ Cl ₂ oxidized with (____) SbCl ₅ at room temperature, (—) and (—) reduced with diethyl amine	60
Figure.4.3.2. UV-visible absorption spectrum of Mn[T(<i>p</i> -OH)PP] in CH ₂ Cl ₂ oxidized with (____) SbCl ₅ at room temperature (—), and (—) reduced with diethyl amine	61
Figure.4.3.3. UV-visible absorption spectrum of Mn[T(<i>o</i> -NO ₂)PP] in CH ₂ Cl ₂ oxidized with (____) SbCl ₅	

at room temperature, (—) and (—) reduced with diethyl amine	62
Figure.4.3.4. UV-visible absorption spectrum of Mn[TpyP] in CH ₂ Cl ₂ oxidized with (—)SbCl ₅ at room temperature, (—) and (—) reduced with diethyl amine	63
Figure.4.5.1. Cyclic voltammogram of Cd[T(2,5-(OCH ₃) ₂)PP] in CH ₂ Cl ₂ Containing 0.1M TBAP at room temperature	65
Figure.4.5.2. Cyclic voltammogram of Cd[T(o-NO ₂)PP] in CH ₂ Cl ₂ Containing 0.1M TBAP at room temperature	66
Figure.4.5.3. Cyclic voltammogram of Cu[T(2,5-(OCH ₃) ₂)PP] in CH ₂ Cl ₂ Containing 0.1M TBAP at room temperature	67
Figure.4.5.4. Cyclic voltammogram of Cu[T(o-NO ₂)PP] in CH ₂ Cl ₂ Containing 0.1M TBAP at room temperature	68
Figure.5.2.1. Effect of Zero field splitting, Energy levels(i)A Triplet state(ii) A quartet state for of an axially symmetric system	76
Figure.5.7.1. (i).X-band ESR spectra of VO[T(o-NO ₂)PP] in CH ₂ Cl ₂ oxidized with SbCl ₅ at room temperature	87
Figure.5.7.1 (ii) A and B.X-band EPR spectra of VO[T(2,5-(OCH ₃) ₂)PP] in CH ₂ Cl ₂ oxidized with SbCl ₅ at room temperature	88
Figure.5.7.1. (iii) A and B.X-band EPR spectra of VO[TpyP] in CH ₂ Cl ₂ Oxidized with SbCl ₅ at room temperature	89
Figure.5.7.1. (iv). A,B and C.X-band EPR spectra of VO[T(p-OH)PP]in CH ₂ Cl ₂ oxidized with SbCl ₅ at room Temperature	90
Figure.5.7.1. (v).Infrared spectra of VO[T(2,5-(OCH ₃) ₂)PP] in CH ₂ Cl ₂ Oxidized with SbCl ₅ at room temperature	91
Figure.5.7.1 (vi) A..UV-visible absorption spectrum of VO[T(2,5-(OCH ₃) ₂)PP] CH ₂ Cl ₂ oxidized with (—) SbCl ₅ at room temperature, (—) and (—) reduced with diethyl amine	92
Figure.5.7.1 (vi) B..UV-visible absorption spectrum of	

VO[T(p-OH)PP] in CH ₂ Cl ₂ oxidized with (—)SbCl ₅ at room temperature, (—), and (—) reduced with diethyl amine	93
Figure.5.7.1 (vi) C..UV-visible absorption spectrum of VO[T(o-NO ₂)PP] in CH ₂ Cl ₂ oxidized with (—)SbCl ₅ at room temperature, (—),and (—) reduced with diethyl amine	94
Figure.5.7.1 (vi) D..UV-visible absorption spectrum of VO[TpyP] in CH ₂ Cl ₂ oxidized with (—)SbCl ₅ at room temperature, (—), and (—) reduced with diethyl amine	95

Preface

Porphyrin chemistry is an old chemistry and is an area which is researched widely, in spite of the voluminous information available. Now porphyrins are synthesized and more new results appear in the literature everyday. This is because porphyrins are not only biologically important but also find their way in the field of medicine and material sciences. Quite a good number of modified and new porphyrin ligands are available in the literature. But metal complexes of such porphyrins are not properly explored. This provides us an opportunity to venture into this field of research. This thesis embodies the physico-chemical studies of some vanadyl porphyrins and manganese porphyrins which are not reported so far in the literature.

This thesis consists of five chapters. Chapter 1 presents a brief review of the EPR and Cyclic voltammetric studies of some vanadyl porphyrins.

Chapter 2 describes different experimental techniques and measurements used in the course of the investigation.

Chapter 3 presents cyclic voltammetric studies of some vanadyl porphyrins.

Chapter 4 deal with cyclic voltammetric studies of some manganese, cadmium and copper porphyrins.

Chapter 5 describes EPR of some substituted vanadyl meso-tetraphenyl porphyrins oxidized with SbCl_5

INTRODUCTION

Metalloporphyrins are not only biologically important class of compounds but find their applications in the field of medicine and material sciences^{1,2}. Some metalloporphyrins are also used as catalyses³ in the oxidation of alkenes. Vanadyl porphyrins are also found in the oil shells⁴, which are believed to be of biological origin and provide valuable molecular fossil record of the past environmental conditions of the geological era. Synthetic porphyrins such as supra molecular porphyrin arrays provide nano scale optical and magnetic materials⁵⁻¹². Such self assembled materials provide the possibilities in the formation of molecular electronic devices. Metalloporphyrin macro cycles are known as molecular binding blocks of one –dimensional molecular metals⁷.

It is well known that metalloporphyrin π -cation radicals exhibit similar properties with that of *chlorophyll a* and B_{chl} ¹⁴⁻²⁰. Occurrence of Fe(II)porphyrins π -cation radicals in cytochromes and heme catabolism are well documented^{21,22}. It is also known that the oxidation of Fe(III)P occur in catalase and peroxidase²³.

Obviously, study of redox properties of metalloporphyrins will give some interesting information. The redox behavior of metalloporphyrins also depends on the ring substitution.

REFERENCES

1. A.J.Crowe, *Tin and its uses*, **162**, 4(1990) and references there in
2. A.J.Crowe, *Tin and its uses*, **163**, 4(1990) and references there in
3. C.-J.Lin, W.-Y.Yu, S.-M.Peng, T.C.W.Mak, C.,M.Che, *J.Chem.Soc.Dalton trans.* **11**, 1805(1998) and references there in
4. J.A.Shelmutt and M.M.Dobry, *J.Phys.Chem.*, **87**(16) 3001(1988) and references there in
5. A.Osuka, M.Ikada, H.Sheratori, Y.Nishimura and I.Yamazuki, *J.Chem.Soc., Perkin trans.2*,1019(1999) and references there in
6. K.Chichak and N.R.Branda, *Chem.Commun.*, 523(1999) and references there in
7. A.Rosa, E.J. Baerends , *Inorg.Chem.*,**32**,5637(1993) and references there in
8. K.Chichak and N.R.Branda, *Chem.Commun.*, 1211(2000) and references there in
9. T.-B.Tsao, G.-H, Lee, C.-Y.Yeh and S.-M.Peng, *Dalton trans.*, 1465(2003) and references there in

10. C.M.Drain, J.D.Batteas, G.W.Flynn, T.Millik, N.Chi, D.G.Yaslon and H.Sommers, Colloquium of Nat.ac.Scie "Nanoscience :underlying physical concepts and phenomena" Washington DC, May 18-20(2000), PNAS early edition and references there in
11. T.E.O.Sereen, K.B.Lawton, N.Dolney, R.Ispasolu, T.Goodson III, S.J.Martin, D.D.C.Bradley, H.LAnderson, *J.Mater, Chem.*, **11**,312(2001) and references there in
12. D.Kim and A.Osuka, *Acc.Chem.Res.*, **32(10)**,375(2004) and references there in
13. R.Harada, H.Okawa, T.Kojima, *Inorg.Chim.Acta.*, **358**, 489(2005) and references there in
14. D.H.Kohl, in" *Biological applications of Electron Spin Resonance*", H.M.Wartz, J.R.Bolton and D.C.Borg.Ed., Wiley-Interscience, New York, N.Y., 1972, p213.
15. J.D.McElory, .Fehar, and D.Mauzerall, *Biochem.Biophys.Acta*, **267**, 363(1972) and references there in
16. W.W.Passon, *Biochem.Biophys.Acta*, **153**,248(1968) and references there in
17. P.A.Loach and K.Walsh, *Biochemistry*, **8**, 1908(1969) and references there in

18. J.R.Bolton, .E.Clayton and D.W.Reed, *Phot.Chem.Photbiol.*,**9**, 209(1969) and references there in
19. J.T.Warden and J.R.Bolton, *J.Am.Chem.Soc.*, **94**, 4351(1972) and references there in
20. D.Dolphin and R.H.Felton, *Acc.Chem.Res.* **7**, 26(1974) and references there in
21. C.E.Castro, *J.Theor.Biolo.*, **33**,475(1972) and references there in
22. (a) N.Sutin, and A.Forman, *J.Am.Chem.Soc.*, **93**,5274(1971) and references there in (b) N.Sutin, *Chem.Brit.*, **8**. 148(1972) and references there in
23. C.A.Reed, in "*Electrochemical and spectrochemical studies of Biological Rex components*", *Advances in Chemistry series*, Edited by K.M.Kadish (American chemical society, Washington.D.C., 1982), 201, p333.

Chapter 1

A brief review of the EPR and cyclic voltammetric studies of some vanadyl porphyrins

This chapter presents a brief review on vanadyl porphyrins of substituted TPP systems mainly focusing on the electron paramagnetic resonance (EPR) and Cyclic voltammetric (CV) studies

1.1. Vanadyl porphyrin

The EPR of the oxidation of VOTPP with $\text{Br}_2/\text{SbCl}_5/\text{TiCl}_4$ are available in the literature¹. The biradical/triplet state generated by SbCl_5 could not be observed by earlier workers even in the glass state. Even the preoxidised complexes could be observed only at low temperatures. The reason for not observing these complexes was attributed to thermodynamic instability of these complexes at room temperature. Observation of smaller hyperfine coupling constant (at low temperature) was attributed to the compression N-V-N bonding due to the additional bonding of $[\text{SbCl}_4]^+$ or $[\text{TiCl}_3]^+$ or Cl^- with the oxygen of vanadyl. Hoshimo et al² could observe the triplet state at 77K. They have generated the triplet state by γ -irradiation. But they also could not observe $\Delta M_s = \pm 1$ transition which they attributed to the intense back ground signal of VOTPP. They have estimated that vanadium atom to be

0.5A° out of plane of porphyrin plane. They also have suggested that VOTPP⁺ to be in ²A_{2u} state.

Later on Tomba³ et al have reported the EPR of VOTPP oxidation with SbCl₅. They could observe the pre-oxidized species at room temperature. Even the triplet state could be observed at room temperature at higher modulation although the signal was quite broad. The formation of mono cation was further supplemented by IR spectra^{4,5}. Further, formation of dication was also observed. On the basis of EPR data they have suggested the possibilities that some species with electron spin density in a_{1u} state co-exist. They also have reported the EPR of VO[T(*m*-NO₂)PP], VOTPP(X_n) (X_n = Br , n= 1 to 4), VO[T(*p*-X)PP] where X = Cl, Br, F, -CH₃ and -OCH₃⁶. The EPR spectra of the oxidation product of these compounds with SbCl₅ exhibit similar pattern to that of the oxidation products of VOTPP. Formations of cations are also supported by IR spectra. No significant changes in the EPR spectra were formed due to peripheral substitution. The average inter electron distance of 3.623±0.030A° is also reported. It has been suggested that some considerable unpaired π-electron density does exist in a_{1u} state although more dominantly in a_{2u} state.

On the other hand cyclic voltammetric studies have shown some considerable change in the oxidation potentials. Electrophilic substitutions in the exo-positions of the pyrrole ring shift the oxidation potentials to more higher side. Substitution in the phenyl ring with electron withdrawing group shift the oxidation potentials to higher side, while substitution with electron donating group in the phenyl ring lower the oxidation potentials.

Normally, metal $d_{xy}/d_{x^2-y^2}$ -porphyrin (a_{1u})/(a_{2u}) interaction do not occur in a planar porphyrin complexes. This is because the metal d-orbitals are orthogonal to porphyrin ligand a_{1u}/a_{2u} HOMOS. Walker and Co-workers⁷ have reported that metal d metal and porphyrin ligand a_{1u}/a_{2u} orbitals can have interactions in ruffle and saddle distortions. Similar view is reported by Gosh et al⁸, existence of such interactions is reported by Harada et al⁹ in vanadyl complexes of octaphenyl porphyrin (VO(OPP)) and vanadyl dodecaphenyl porphyrin(VO(DPP)). They have observed that porphyrin with saddle distortion undergoes disproportionation on oxidation. This is due to destabilization of a_{1u} leading to accidentally degenerated with a_{2u} . Thus, a_{1u} type cation radical is unstable and disproportionated into dication and neutral species. Thus, HOMO-LUMO gap narrowing down is observed in the voltammogram. They further pointed out that in vanadyl

porphyrins (VO(DPP)) due to ligand distortion a_{1u} orbital elevate leading to the narrowing of HOMO-LUMO gap. This narrowing is observed in lowering of the oxidation potentials in the voltammogram.

REFERENCES

1. G.E.Selyutin, A.A.Shklyayev and V.F.Anufrieko, *Dokl.Akad.Nauk.SSR*, **255**,390(1980) and references there in
2. M.Hoshino, S.Konishi, M.Imamura, S.Watanabe and Y.Hama, *Chem.Phys.Lett*, **102**,259(1983) and references there in
3. A.Tomba Singh and A.Lemtur, *Spectrochim.,Acta Part A*, **59**, 1549(2003) and references there in
4. E.T.Shimomura, M.A.Phillippi, H.M.Goff, W.F.Schulz and C.A.Reed, *J.Am.Chem.Soc.***103**, 6778(1981) and references there in
5. A.S.Hinman, B.J.Pavelich and K.McGarty, *Can.J.Chem.*, **66**, 1589(1988) and references there in
6. A.Tomba Singh, *Ph.D Thesis*,(2002) and references there in
- 7 (a) G.Simonneaux, V.Schunemann, C.Morice, L.Carel, L.Toupet, H.Winker, A.X.Trautwein, and F.A.Walker, *J.Am.Chem.Soc.*, **122**, 43666(2000) and references there in
(b) M.K.Safo, M.J.N.Nesset, F.A.Walker, P.G.Debrunner, and W.R.Scheidt, *J.Am.Chem.Soc.*, **119**,9438(1997) and references there in
(c) F.A.Walker, H.Nasri, I.Turowskatyrk, K.Mohanrao, C.T.Watson, N.V.Shokhirew P.G.Debrunner and W.R.Scheidt, *J.Am.Chem.Soc.***118**,12109(1996) and references there in

(d) M.R.Safo, and F.A.Walker., *J.Am.Chem.Soc.*, **118,7373**(1996)

and references there in

(e) M.K.Safo, F.A.Walker, A.M.Raitsimring, W.P.Walters,
D.P.Dolata, P.G.Debrunner, and W.R.Scheidt ..,
J.Am.Chem.Soc., **116**, 7760(1992) and references there in

(f) M.K.Safo, G.P.Gupta, C.T.Watson, U.Simonis, F.S.Walker
and W.R.Scheidt., *J.Am.Chem.Soc.*, **114**,7066(1992) and
references there in

8 (a).A.Ghosh, I.Halvorsen, H.J.Nilsen, E.Steene,
T.Wondimagegin, R.Lie, E.Vancaemelbacke, N.Guo, Z.Ou,
and M.K.Kadish., *J.Phs.Chem.B.*, **105**,8120(2001) and
references there in

(b) A.Ghosh, E.Gonzalez, and T.Vangberg.,
J.Phys.Chem.B, **103**, 1363(1999) and references there in

9 R.Harada, H.Okawa and T.Kojima., *Inorg.Chim.Acta.*, **358**,
489(2005) and references there in

Chapter-2

Experimental Section

2.1. Introduction

This chapter deals with the general experimental techniques and the synthesis of porphyrin and metalloporphyrins, purification of solvents and other reagents used in cyclic voltammetric and ESR studies.

2.2 Solvents

Common solvent and other reagents used at various stages of this work were purified according to the standard procedures described¹.

1) Chloroform: Drum samples were dried over CaCl_2 and distilled twice before being employed for synthesis, extraction and running column. For recrystallization and other physical measurements spectroscopic grade solvent was used.

2) Dichloromethane: Drum sample were refluxed over K_2CO_3 (anhydrous) for about 4 hours and distilled. This solvent has been used for synthesis, extraction and running column. For recrystallization and other physical measurements spectroscopic grade solvent was used

3) Methanol: Drum samples were refluxed over CaO (anhydrous) for about 6 hours and distilled with iodine and Mg turnings twice.

This solvent has been used for synthesis, extraction and running column. For recrystallization and other physical measurements spectroscopic grade solvent was used

4) Pyrrole: Pyrrole was purified by distillation under reduced pressure in the presence of KOH pellets and stored in a dark sealed bottle.

2.3. Oxidizing agent

Antimony pentachloride solution (1M solution in dichloromethane) was purchased from Aldrich Chemical Company and used directly.

2.4. Reagents and supporting electrolytes^{2,3}

This section describes the methods of preparation of tetra-n-butylammonium perchlorate(TBAP)¹ and the complexes which were used during the course of our investigation. Some of the reagents were procured commercially.

i) Sodium perchlorates

Sodium perchlorate has been prepared² by neutralization of sodium carbonate(AnaIR) with hydrogen perchloric acid(Qualigen, AR). After complete neutralization, the volume of the reaction mixture was concentrated and allowed to cool and sodium perchlorate crystallizes out. It was then recrystallized from distilled

water, several times. The purity of the sample has been tested by running a cyclic voltammogram.

ii) Tetra-n-butylammonium perchlorate (TBAP)

A saturated solution of tetrabutylammonium iodide (Aldrich Chemical Company) has been prepared in distilled water. To this solution, sodium perchlorate was added, while tetrabutylammonium perchlorate precipitates out instantly. It has been stirred constantly till the formation of the precipitate and filtered fast. In order to avoid the liberation of iodine excess of sodium perchlorate was added. The precipitates have been suction filtered and dried by pressing between filter papers. After complete drying, tetrabutylammonium perchlorate was dissolved in methanol and reprecipitated out by adding distilled water. It was then filtered and dried as before, then recrystallized from methanol. Glassy crystals were formed. The purity of the sample has been tested by running a cyclic voltammogram.

2.5. Synthesis of Porphyrins

2.5.1. meso-5,10,15,20-Tetrakis(2,5- methoxyphenyl)porphyrin

meso-5,10,15,20-Tetrakis(2,5-dimethoxyphenyl)porphyrin⁴ was prepared according to the method as described in the literature. In a 500 mL round bottom flask fitted with nitrogen bubbler 2,5-dimethoxy benzaldehyde(0.4952g, 2.98 mmol) and



pyrrol(210 μ l, 2.98 mmol) were dissolved in 300 mL of dichloromethane. After purging nitrogen for 10 min, the condensation of 2, 5-dimethoxy benzaldehyde and pyrrole was initiated by adding catalytic amount of $\text{BF}_3 \cdot \text{OEt}_2$ (120 μ l, of 2.5M stock solution). The reaction mixture was stirred at room temperature for 1 hour. The progress of the reaction was monitored by taking aliquots of the reaction mixture at regular intervals and oxidizing with p-chloranil and recording the absorption spectra which clearly confirmed the formation of porphyrin. After 1 hour p-chloranil (0.7327g, 2.98 mmol) was added and the reaction mixture was stirred in air for additional 1 hour. The solvent was removed under reduced pressure and the crude compound was purified by silica gel column chromatography using dichloromethane.

λ_{max} : 419 nm(S), 513nm, 546nm, 587nm, 642nm

2.5.2.meso-5,10,15,20-Tetrakis(o-nitrophenyl)porphyrin

meso-5,10,15,20-Tetrakis(o-nitrophenyl)porphyrin was prepared according to the method as described in the literature⁴.

λ_{max} : 421 nm(S), 516nm, 551nm, 593nm, 649nm

2.5.3.meso-5,10,15,20-Tetrakis(p-hydroxyphenyl)porphyrin

meso-5,10,15,20-Tetrakis(p-hydroxyphenyl)porphyrin was prepared according to the method as described in the literature⁵.

To a solution containing 18.3180g (150 mmol) of p-hydroxy benzaldehyde in 300 ml propionic acid 13.5 mL (106 mmol) of propionic anhydride were added. The resulting solution was allowed to reflux with stirring under the protection of bubbled nitrogen. Then 10.40 mL (150 mmol) of freshly distilled pyrrole in 10 mL of propionic acid was added drop wise. After the addition the reaction mixture was stirred for further 30 min, and then 300 mL of 90% ethanol was added under vigorous stirring. The mixture was cooled to room temperature and kept at 15°C overnight. The tarry mixture was filtered and the solid product was washed repeatedly with a mixture of ethanol and propionic acid (1:1 in volume), then with hot water until the rinsed solution were no longer dark. The filter cake was dried in air overnight, then at 150°C for 2 hour. The purple coloured crystalline meso-5, 10,15,20-Tetrakis(p-hydroxyphenyl)porphyrin were obtained. .

λ_{\max} : 421 nm(S), 518nm, 555nm, 593nm, 649nm

2.5.4.meso-5,10,15,20-Tetrakis(pyridyl)porphyrin

meso-5,10,15,20-Tetrakis(pyridyl)porphyrin was purchased from Sigma-Aldrich chemical and was used directly.

2.6. Synthesis of metalloporphyrins

2.6.1. Vanadyl porphyrins VO[T(2,5-(OCH₃)₂)PP]⁶

The reaction was carried out with a mixture of 13.5 mL of glacial acetic acid, 6.5 mL of pyridine, 297mg(1.37mmol) of vanadyl sulphate and 358.21mg(0.42mmol) meso-5,10,15,20-Tetrakis(2,5-dimethoxyphenyl)porphyrin [T(2,5-(OCH₃)₂)PP] were taken in a 100 mL round bottom flask and was refluxed until the reaction was essentially complete (usually 4 to 5 hour). The crude product was cooled and washed with water thrice and the crude compound was purified by running through a silica gel column using dichloromethane.

VO[T(*o*-NO₂)PP], VO[T(*p*-OH)PP] and VO[TpyP] were prepared according to the above method given in the literature⁶.

VO[T(2,5-(OCH₃)₂)PP]

λ_{\max} in dichloromethane : 425 nm, 546nm

VO[T(*o*-NO₂)PP]

λ_{\max} in dichloromethane: 426 nm, 551 nm

VO[T(*p*-OH)PP]

λ_{\max} in dichloromethane: 428 nm, 550 nm

VO[TpyP])

λ_{\max} in dichloromethane: 420 nm, 545 nm.

2.6.2. Manganese porphyrins Mn[T(2,5-(OCH₃)₂)PP]⁶

The reaction was carried out with a mixture of 335mg(1.37mmol) of manganese (II) acetate in methanol and 358.21mg(0.42mmol) of meso-5,10,15,20-Tetrakis(2,5-dimethoxyphenyl)porphyrin [T(2,5-(OCH₃)₂)PP] in chloroform. The solution was taken in a 100 mL round bottom flask and refluxed until the reaction was essentially completed, usually around 5 hour. The Crude product was cooled and washed with water thrice, the crude compound was purified by running a silica gel column chromatography using dichloromethane.

Mn[T(*o*-NO₂)PP], Mn[T(*p*-OH)PP] and Mn[TpyP]) were prepared according to the above method given in the literature⁶.

Mn[T(2,5-(OCH₃)₂)PP]

λ_{\max} in dichloromethane : 411 nm. 480nm (Soret), 575 nm, 607 nm

Mn[T(*o*-NO₂)PP]

λ_{\max} in dichloromethane: 414 nm. 480nm (Soret), 584 nm, 620 nm

Mn[T(*p*-OH)PP]

λ_{\max} in dichloromethane: 417 nm. 480nm (Soret), 585 nm, 623 nm

Mn[TpyP])

λ_{\max} in dichloromethane: 417 nm. 475nm (Soret), 575 nm, 609 nm.

2.6.3. Cadmium and copperporphyrins⁶

Cd[T(2,5-(OCH₃)₂)PP]

The reaction was carried out with a mixture of 335mg(1.37mmol) of cadmium (II) acetate in methanol and 358.21mg(0.42mmol) of meso-5,10,15,20-Tetrakis(2,5-dimethoxyphenyl)porphyrin [T(2,5-(OCH₃)₂)PP] in chloroform. The solution was taken in a 100 mL round bottom flask and refluxed until the reaction was essentially completed, usually around 5 hour. The Crude product was cooled and washed with water thrice, the crude compound was purified by running a silica gel column chromatography using dichloromethane.

Cd[T(*o*-NO₂)PP], Cu[T(2,5-(OCH₃)₂)PP] and Cu[T(*o*-NO₂)PP] were prepared according to the above method given in the literature⁶.

Cd[T(2,5-(OCH₃)₂)PP]

λ_{\max} in dichloromethane : 427 nm. 549nm

Cd[T(*o*-NO₂)PP]

λ_{\max} in dichloromethane: 429 nm, 555 nm

Cu[T(2,5-(OCH₃)₂)PP]

λ_{\max} in dichloromethane : 422 nm. 542nm

Cu[T(*o*-NO₂)PP]

λ_{\max} in dichloromethane: 424 nm, 556 nm

2.7. Instrumentation

2.7.1. Electron Paramagnetic Resonance (EPR)

EPR measurements were done using JEOL JES TE100 EPR spectrometer working at X band frequencies having 100 kHz field modulation at Pondicheery University, Pondicheery.. Oxidation was carried out in ESR tube by dropping SbCl_5 . All measurements were done after deaerating by bubbling nitrogen gas through the solution in the tube. The g values were determined by using DPPH reference ($g = 2.0036$).

2.7.2. Cyclic voltammetric measurements

Redox potentials were determined using CHI 620B Electrochemical Analyzer. The electrolytic cell is comprised of the following. A CHI(102) platinum electrode was used as a working electrode. An Ag/AgCl electrode was employed as a reference electrode. A platinum wire was used as an auxiliary electrode. Dry dichloromethane was used as the solvent. The amount of 0.1M of tetra-n-butylammonium perchlorate (TBAP) was used as supporting electrolyte. The solvent in the electrolyte cell was deaerated with oxygen free dry nitrogen gas before any measurement had been done and nitrogen blanket above the solution has been maintained. Calibration of $E_{1/2}$ values and

diffusion current were made by using a known concentration of pure ZnTPP in dichloromethane/TBAP (0.1M) medium.

2.7.3. UV spectroscopy

Absorption spectroscopy was measured by BECKMAN 650DU Spectrophotometer. Visible spectrums were measured in between the range 350-750 nm. Oxidations were carried out in quartz cuvette by dropping SbCl_5

References

1. A.I.Vogel, *A text book of practical organic Chemistry*, fourth Edition [ELBS] Longman, London, 1978
2. *Hand book of Preparative Inorganic Chemistry*, Edited by G.Brauer (Academic press, New York, 1965), **Vol.II**. pp1185.
3. *Inorganic Synthesis*, Editor-in-Chief: Therald Moellur (McGraw Hill, 1975), **Vol.5**, pp154.
4. (a) I.Gupta, and M.Ravikanth., *Tetraheron*, **59**, 6131(2003),
(b) I.Gupta, and M.Ravikanth., *Tetr.Lett*, **43**,9453(2002),
(c) J.S.Lindsey, H.C.Hsu, and I.C.Schreimen., *Tetra.Lett.*, **27**,4969(1989),
(d) R.W.Wagner, D.S.Lawrence, and J.S.Lindsey., *Tetra.Lett.*, **28**, 3069(1987).
5. Z.Jing, G.Yang, C.Shaokui, Z.Wennan, and W.Dongmai., www.chemistry.maq.org/cij/2002/048039.htm. **8**,39(2002).
6. J.S.Erdman, V.G.Ramsey, N.W.Ka;emda, and W.E.Hanson., *J.Am.Chem.Soc.*,**78**,5844(1956). b) A.D.Alder, F.R.Longo, F.Kampas, and J.Kim., *J.Inor.Nucl.Chem.*, **32**,2443(1970).

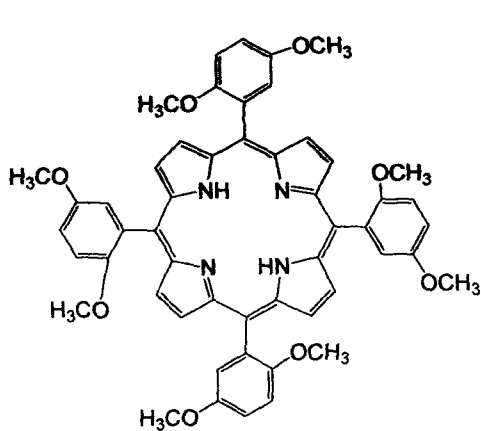
CHAPTER 3

CYCLIC VOLTAMMETRIC STUDIES OF SOME VANADYL PORPHYRINS

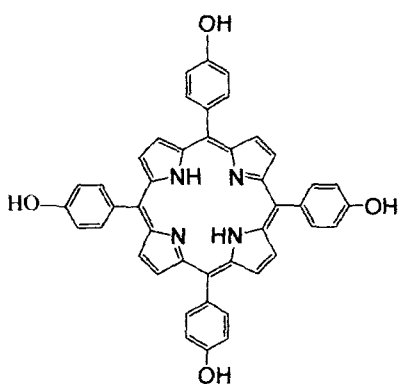
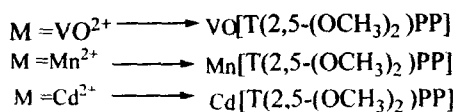
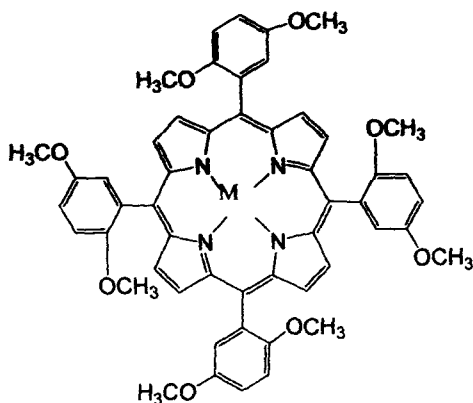
3.1. INTRODUCTION

Cyclic voltammetry has been used extensively in unlocking the redox processes in porphyrin and metalloporphyrin systems. The structure of the free base porphyrin and metalloporphyrins are presented in figure.3.1.1a and fig.3.1.1.b. The success of the cyclic voltammetric study in porphyrins and metalloporphyrins is reflected in the volume of research papers published in the literature¹⁻⁸. We present here a brief introduction of the electrochemical behavior of some metalloporphyrins (in general). One can tune to the variation in the redox potentials of metalloporphyrins depending on the peripheral substituents and the central metal atom.

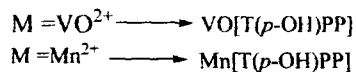
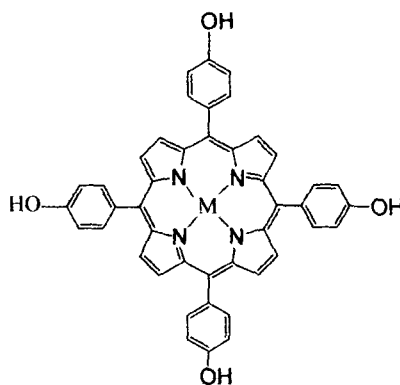
Generally, a metalloporphyrin may possess D_{4h} or C_4 symmetry (ordinarily). The HOMO (Highest occupied molecular orbital) a_{1u} , a_{2u} is nearly degenerate while the LUMO (Lowest unoccupied molecular orbital) e_g is truly degenerate. On oxidation electrons are removed from the HOMO levels. The redox process may



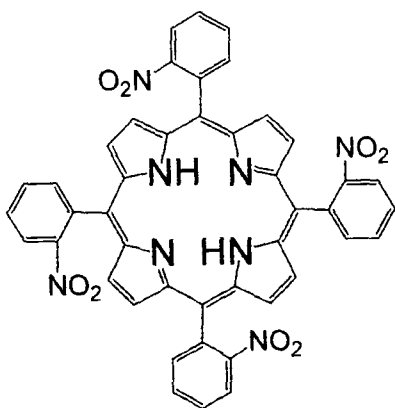
meso-5,10,15,20-Tetrakis(2,5-dimethoxyphenyl)porphyrin
[T(2,5-(OCH₃)₂)PP]



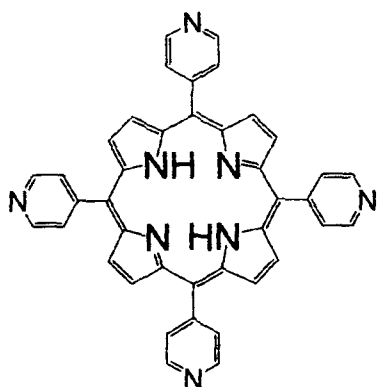
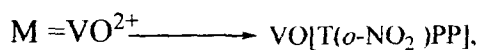
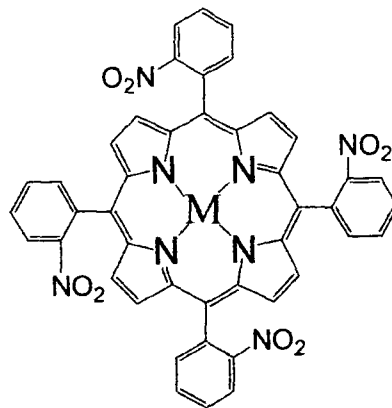
meso-5,10,15,20-Tetrakis(*p*-hydroxyphenyl)porphyrin
[T(*p*-OH)PP]



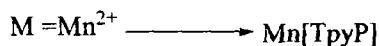
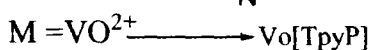
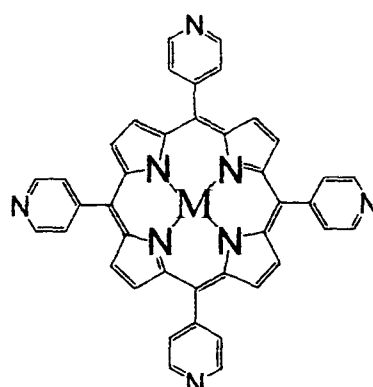
3.1.1a. Structure of free base porphyrin and metalloporphyrin



meso-5,10,15,20-Tetrakis(*o*-nitrophenyl)porphyrin
[T(*o*-NO₂)PP].



meso-5,10,15,20-Tetrakis(pyridyl)porphyrin
[TpyP]

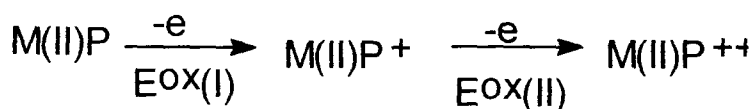


3.1.1b. Structure of free base porphyrin and metalloporphyrin

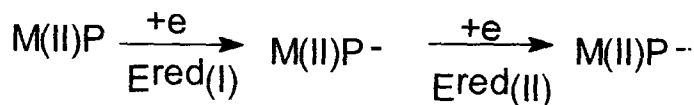
occur (i) in the porphyrin ligand or (ii) in the central metal atom or (iii) in both systems. The first processes occur when the central metal atom is electro inactive to the redox process such a Zn, Cu

etc. The second and the third processes occur when the central metal atom is electro active to the redox process such as Fe, Co, Mn etc. One can understand by considering the occupied energy levels of π - electrons of the ligand and the d electrons of the metal atom (fig.3.1.2). In case (i) the HOMO energy level of the porphyrin ligand is higher than that of the metal. Hence the electron transfer will take place on the ligand. In case (ii) the HOMO of the metal atom is higher than that of the ligand. In case (iii) both ligand and metal atom energy levels are more or less same. Hence the electron transfer will take place in both systems. In this thesis we will focus mainly on the vanadyl porphyrins which falls under case(i) redox process of a metalloporphyrins containing a bivalent metal, one can represent as follows¹:

Oxidation



Reduction



$$\Delta_{ox} = E^{ox(II)} - E^{ox(I)}$$

$$\Delta_{red} = E^{red(II)} - E^{red(I)}$$

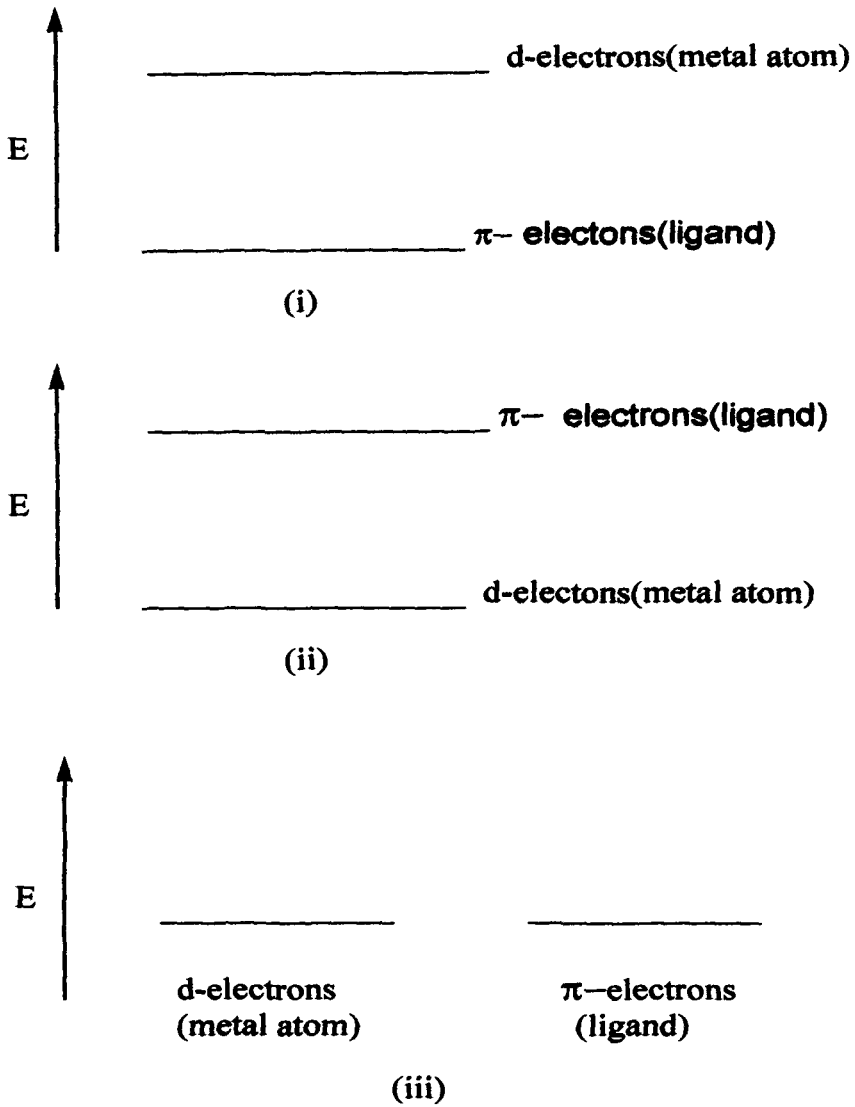


Fig.3.1.2.HOMO representation for metalloporphyrins

For redox processes in the ring, it has been observed that either Δ_{ox} or Δ_{red} are observed to be more or less constant.

$$\Delta_{\text{ox}} \approx 0.3\text{eV}$$

$$\Delta_{\text{red}} \approx 0.5\text{eV}$$

Also, the quantity,

$\delta = E_{\text{ox}} - E_{\text{red}}$ (1) has been observed to be more or less constant for a variety of metalloporphyrins ($2.00 \pm 0.15\text{V}$) although the absolute magnitude of the potentials vary widely. Independence of Δ_{ox} , Δ_{red} and δ of the metal is explained in terms of negligible mixing of the metal orbitals and the orbitals of the porphyrin ligand. The metal ion exerts an inductive columbic effect on the ligand π orbitals through σ frame work. This influence affects only the absolute values of π energy levels but not the relative values ie, the difference in the energies between HOMO and LUMO, using Parise-Parr-Pople π electron energies, the values Δ_{ox} , Δ_{red} and δ have been estimated which agree reasonably well with the corresponding experimental data but fails to correlate when redox processes occur in the metal center.

3.2. PRINCIPLE OF CYCLIC VOLTAMMETRY⁹⁻¹²

It is an electrochemical techniques used as an analytical technique to determine the redox potentials. The electrolytic cell comprises of three electrodes (fig.3.2.1) the working electrode (a platinum discs electrode), an auxiliary electrode (a platinum wire) and a saturated calomel electrode or Ag/AgCl electrode as reference electrode. The working electrode is scanned with a triangular wave (fig.3.2.2.) potential. The triangular wave potential can be arbitrarily fixed between an initial and a final potential which are called switching potentials. Normally, a current-voltage curve known as voltammogram is obtained in an unstirred solution containing a supporting electrolyte and the sample.

For a single-step reversible electron transfer process a voltammogram containing two peaks one on the oxidation side (E^{ox}) and its corresponding reduction.

Peak (E^{red}) on the reverse side is obtained. These two peaks together are called a couple. One can represent a simple redox system by equation.



While sweeping the working electrode with a positive triangular wave, a peak is obtained at a potential E_a ($\approx E^{ox}$)

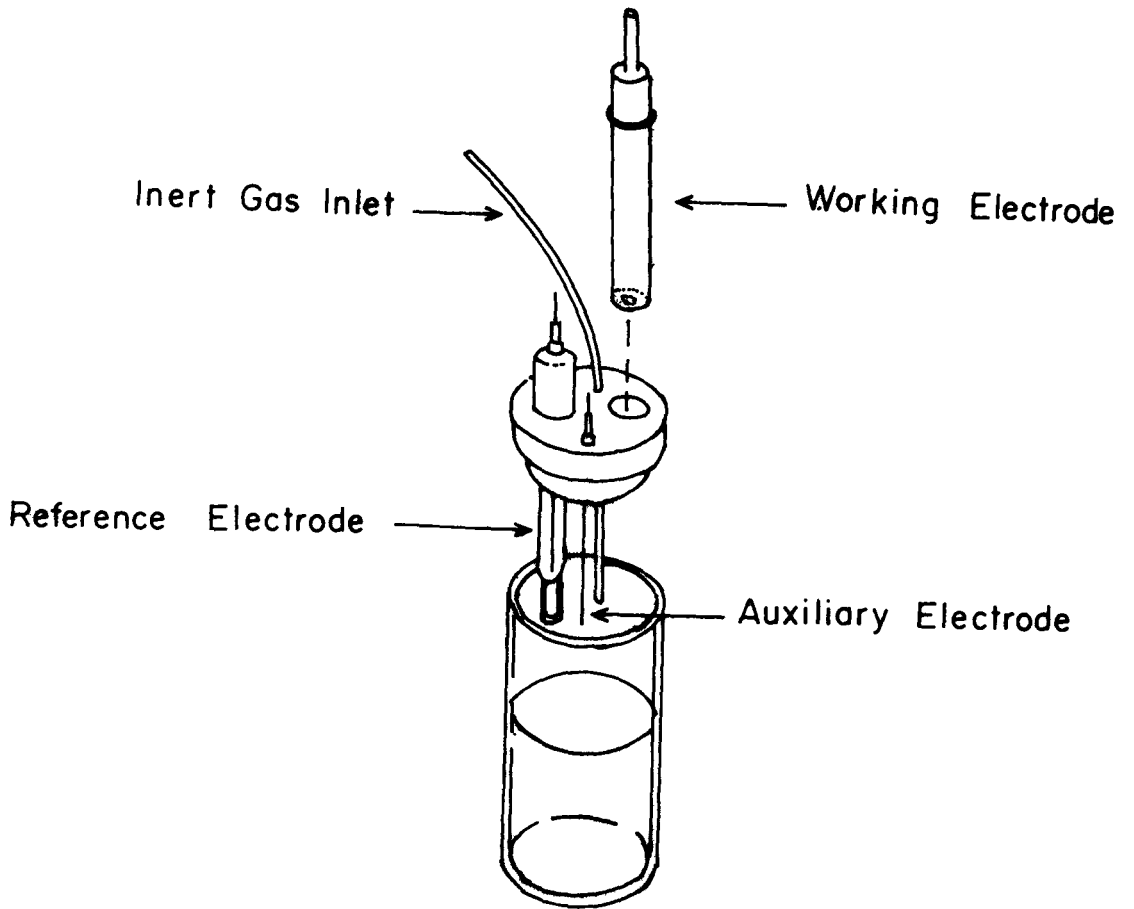


Fig.3.2.1. Electrochemical cell for quality cyclic voltammetry experiment

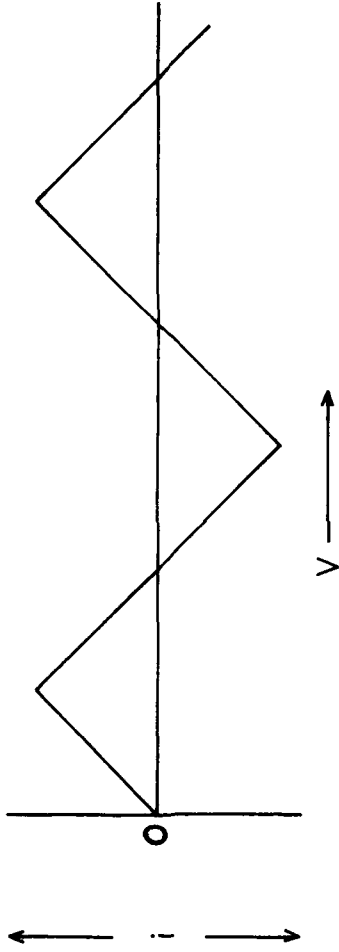


Fig.3.2.2. Triangular wave

corresponding to the process $R \rightarrow R^+$. In the reverse sweep the species R^+ is reduced back to R giving rise to the corresponding reduction peak at a potential $E_c (=E^{red})$. The half-wave potential is given by the expression

$$(E_a + E_c)/2 = E_{1/2} \text{-----} (3.2.2)$$

Expressing in terms of polarographic half-wave potential

$$\begin{aligned} E_p &= E_{1/2} - 1.11(RT/nF) \\ &= E_{1/2} - 1(0.0285/nF) \text{-----} (3.2.3) \end{aligned}$$

where n = number of electron involved in the electrode reaction

$$T = 298 \text{ K}$$

Peak to peak difference

$$\Delta E = E_a - E_c = (0.059/n)V \text{-----} (3.2.4)$$

at 25°C

The peak current for a reversible process is given by Randles-Sevick equation

$$I_p = 2.69 \times 10^5 n^{3/2} A C D^{1/2} \gamma^{1/2} \text{-----} (3.2.5)$$

Where γ is the scan rate in volts per second.

Thus, for a reversible process

$$I_c/I_a = 1 \text{-----} (3.2.6)$$

Where I_c = Cathodic peak current

I_a = anodic peak current

3.3. EXPERIMENTAL DETAILS

The synthesis of meso porphyrin [T(2,5-(OCH₃)₂)PP], [T(o-NO₂)PP], [T(p-OH)PP], TPpP and its vanadyl complexes are discussed in detail in chapter II. Dichloromethane and tetra-n-butylammonium perchlorate were used as solvent and supporting electrolyte respectively. Cyclic voltammetric studies were done on vanadyl porphyrins [VO[T(2,5-(OCH₃)₂)PP], VO[T(o-NO₂)PP], VO[T(p-OH)PP], and VO[TPpP]. All the CV measurements were done with 10⁻³ M solutions of the metalloporphyrins.

Note: Nitrogen gas is bubbled through the electrolytic solution before recording to expel the dissolved oxygen. Nitrogen blanket is maintained above the solution while recording the voltammogram.

3.4. RESULTS AND DISCUSSION

3.4.A. RESULTS

All CV results are summarized in the table (3.1)

VO[T(2,5-(OCH₃)₂)PP] The voltammogram shows two redox couples (fig.3.4.1) with their E_{1/2} values 1.042V and 1.225V respectively. The first oxidation occurs at 1.085V and its corresponding reduction occurs at 0.999V. Its ΔE value is 0.086V. The second oxidation occurs at 1.2744V and its corresponding

reduction occurs at 1.1749V. Its ΔE value is 0.0995V. The current ratio $I_a/I_c \approx 1$

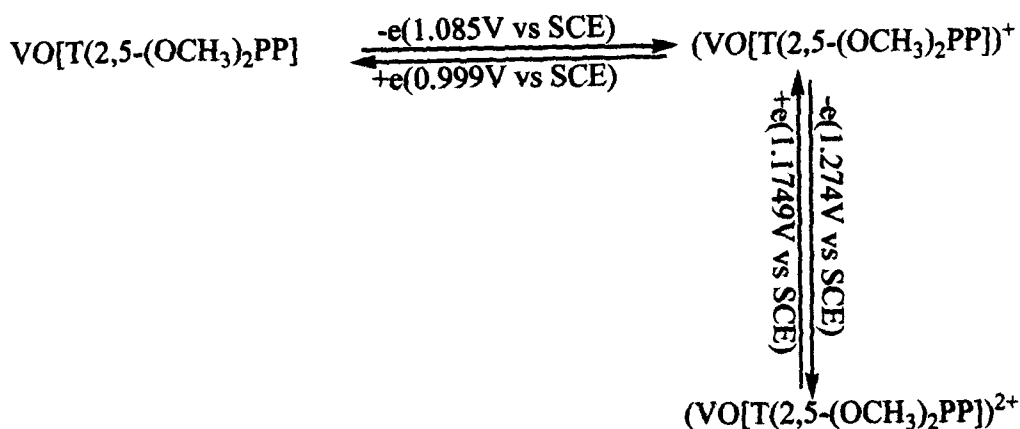
VO[T(*p*-OH)PP], The voltammogram(fig.3.4.2) exhibit the first oxidation at 0.6372V with its corresponding reduction at 0.4745V. Its ΔE value is 0.1627V, $E_{1/2} = 0.5559V$ and $I_a/I_c \approx 1$. The second oxidation occurs at 1.2852V while its corresponding reduction occurs at 0.9482V. The $E_{1/2}$ value is 1.1167V, $\Delta E = 0.337V$ and its $I_a/I_c > 1$.

VO[T(*o*-NO₂)PP], The voltammogram exhibit some additional peaks(fig.3.4.3) otherwise contain regular redox couples which are expected. The first oxidation occurs at 0.730V with its corresponding reduction at 0.553V. The $\Delta E = 0.177V$, $E_{1/2} = 0.6415V$ and its $I_a/I_c \approx 1$. The second oxidation occurs at 1.2271V with its corresponding reduction peak at 1.055V. Its $\Delta E = 0.1721V$, $E_{1/2} = 1.1411V$ and $I_a/I_c \approx 1$.

VO[TPyP] : The voltammogram comprises of two redox couples. The first oxidation occurs at 0.6896V with its corresponding reduction at 0.5185V. The second oxidation peak occurs at 1.0484V with its corresponding reduction peak at 0.8976V (fig.3.4.4)

3.4. B. DISCUSSION

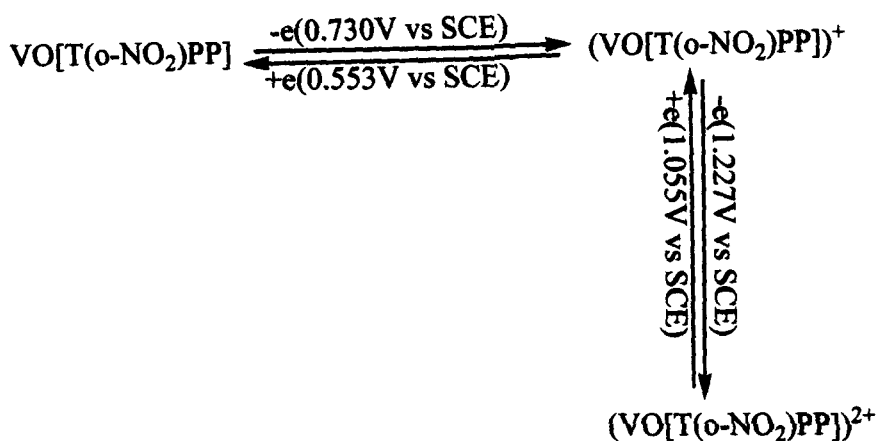
The voltammogram of [VO[T(2,5-(OCH₃)₂)PP] indicate the oxidation potentials are slightly higher than that of the VOTPP by about 0.085V and 0.054V respectively. But the oxidation potentials are slightly lower than that of the [VO[T(*m*-OCH₃)PP] by about 0.075V and 0.076V and to that of the [VO[T(*p*-OCH₃)PP] by about 0.075V and 0.076V. The reason for lowering the oxidation potentials in the case of [VO[T(2,5-(OCH₃)₂)PP] may be because of symmetrical substitution of the phenyl ring which puts it more or less in the similar geometry to that of VOTPP. Although the shifts in the potential either way are small and they are quite uniform. This gives us some thoughts to suggest that there are some changes in the geometry of the molecule on substitution which affect the energy levels (HOMO) of the molecule hence shifts in the redox potentials occurs. However, to supplement this point it requires rigorous theoretical and experimental works which is not possible for us to do at the moment. Perhaps, this is due to the interaction of metal d-orbital and the porphyrin ligand orbital in ruffle and saddle distortion as suggested by Walker et al¹³ and Gosh et al¹⁴ In fact the voltammogram is of successive one electron transfer of the porphyrin ligand and are reversible. The redox process is represented by the following scheme:



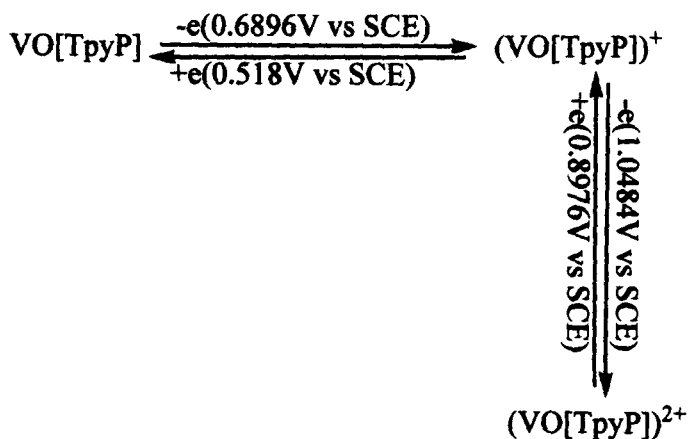
The voltammogram of the VO[T(*p*-OH)PP] is not a straight forward successive one electron transfer process. The first oxidation potential and its corresponding reduction potential are lower than that of VOTPP, while the second oxidation shows very strong oxidation peak current. The peak current corresponds to more than one electron transfer. Similar trends were observed in the case of ZnTDP by earlier workers. Clearly, the second oxidation involved a process which is irreversible along with the reversible process. Evans et al¹⁵ indicated it as due to formation of secondary oxidation states involving the phenolic groups. Murray and his co-workers¹⁶ attributed it as due to oxidative electro polymerizations. On subsequent scanning the peak current decreases leading to film formation at the electrode (fig.3.4.2). The electron donating group (-OH) increases the electron density

of the macrocycle. This makes the removal of electron easier. Thus, the oxidation potential decreases.

The redox process of VO[T(*o*-NO₂)PP] is in line with the redox process of the VO[T(2,5-(OCH₃)₂)PP]. The first oxidation occurred at a lower potential than that of the VOTPP. This is quite surprising because we expected it to occur at a higher potential. The electron withdrawing -NO₂ should make the ring π-electron density lower making oxidation more difficult. This is what we observed in our earlier work¹⁷ in VO[T(*m*-NO₂)PP]. One possible reason could be, the -NO₂ in meta position which is in more sterically hindered position making it more strain to take part in the porphyrin ring resonance. Thereby, no effective electron withdrawal from the ring. The result is no shift in potential to a higher value. This requires more experimental investigations to prove the point. However, the system undergoes two successive oxidation processes involving one electron transfer in each step which is represented as follows:



VO[TpyP] undergo oxidation in the similar steps to that of the VOTPP oxidation. The oxidation potentials are lower than that of the VOTPP. The substituents enriches the π -electron density making oxidation more easier. The oxidation process is represented as



3.5. CONCLUSION

From the results of the cyclic voltammetric investigation of VO[T(2,5-(OCH₃)₂)PP], VO[T(o-NO₂)PP], VO[T(p-OH)PP], and VO[TPyP] we put forward the following observations:

When the metal centre is non electro-active such as vanadyl the redox process takes place in the porphyrin ligand system.

When substitutions in the phenyl ring of the porphyrin ligand are symmetrical with electron donating group, the oxidation potentials are further lowered. The reverse is also true.

It seems the substitution in the ortho-position of the phenyl ring of the porphyrin ligand is more sterically hindered and strain that the substituents do not contribute much to the resonance. Thus, the oxidation potentials of the VOTPP or slightly less (may be due to more puckered structure).

Substitution on the phenyl ring causes distortions which affect the redox potentials.

It is must be likely that the lower in oxidation potentials is due to metal d_{xy} porphyrin orbital (a_{2u}) in ruffle distortion and metal dx^2-y^2 porphyrin orbital (a_{2u}) in saddle distortion.

In some cases such as VO[T(p-OH)PP] secondary electrode reaction takes place resulting in the film formation on surface of the electrode.

Table: 3.1. Cyclic voltammetric data for vanadyl porphyrins at room temperature

Solvent : Dichloromethane

Supporting electrolyte : TBAP

Concentration : 10^{-3} M

Reference electrode : Ag/AgCl

System	Scan Rate (V/s)	Epa(1) V	Epa(2) V	Epc(1) V	Epc(2) V	$\Delta E(1)$ (Epa-Epc) V	$\Delta E(2)$ (Epa-Epc) V	$E_{1/2}(1)$ [(Epa+Epc)/2] V	$E_{1/2}(2)$ [(Epa+Epc)/2] V
VO[T(2,5-(OCH ₃) ₂)PP]	0.06	1.085	1.2744	0.999	1.1749	0.086	0.0995	1.0420	1.2246
VO[T(p-OH)PP]	0.05	0.6372	1.2852	0.4745	0.9482	0.163	0.3370	0.5559	1.1167
VO[T(o-NO ₂)PP]	0.1	0.730	1.2271	0.553	1.055	0.177	0.1721	0.6415	1.1411
VO[TPyPP]	0.01	0.6896	1.0484	0.5185	0.8976	0.171	0.1508	0.6040	0.9730

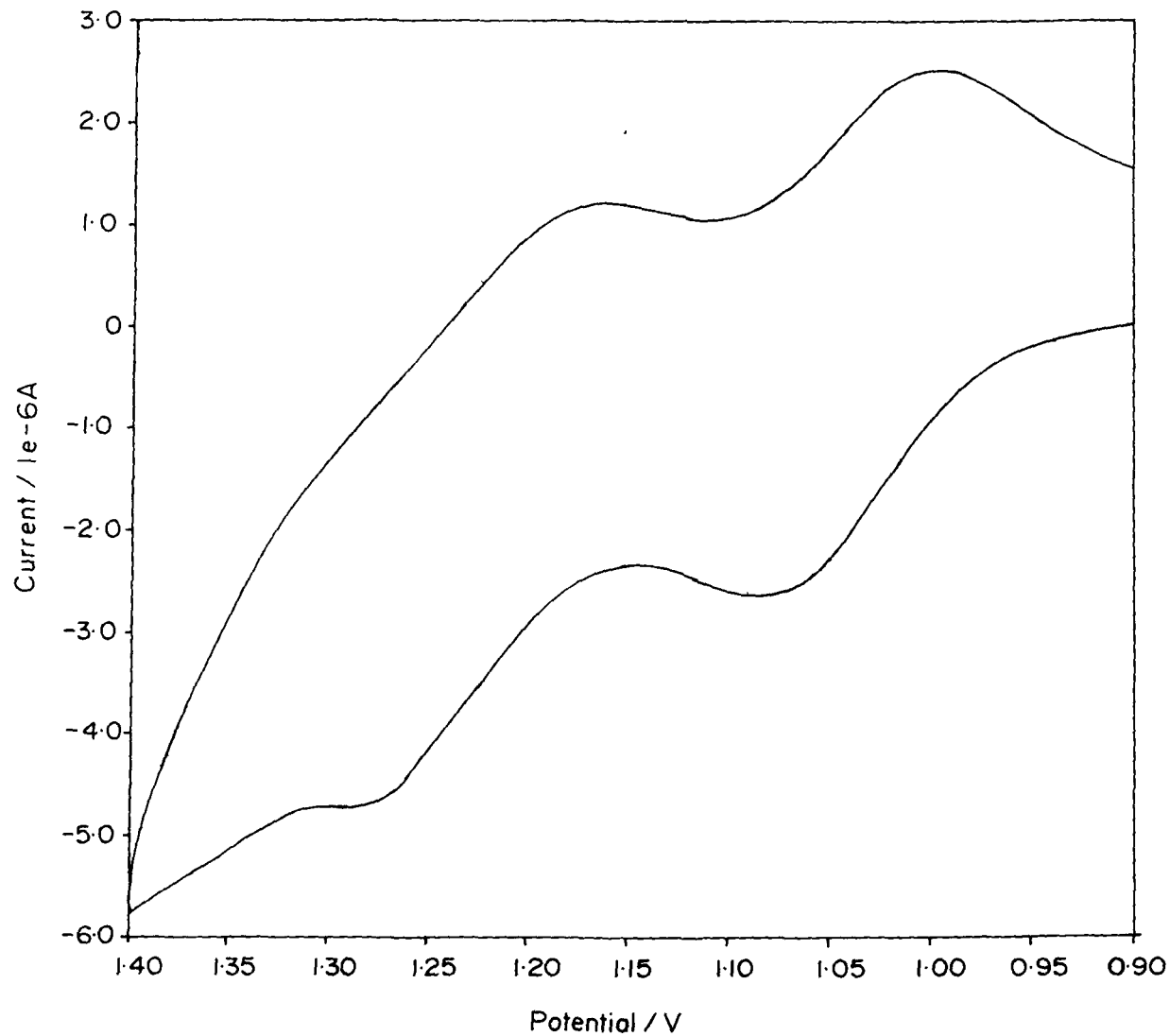


Fig. 3.4.1. Cyclic voltammogram of VO[T(2,5-(OCH₃)₂)PP] in CH₂Cl₂ containing 0.1M TBAP at room temperature. Scan rate 0.06 V/s.

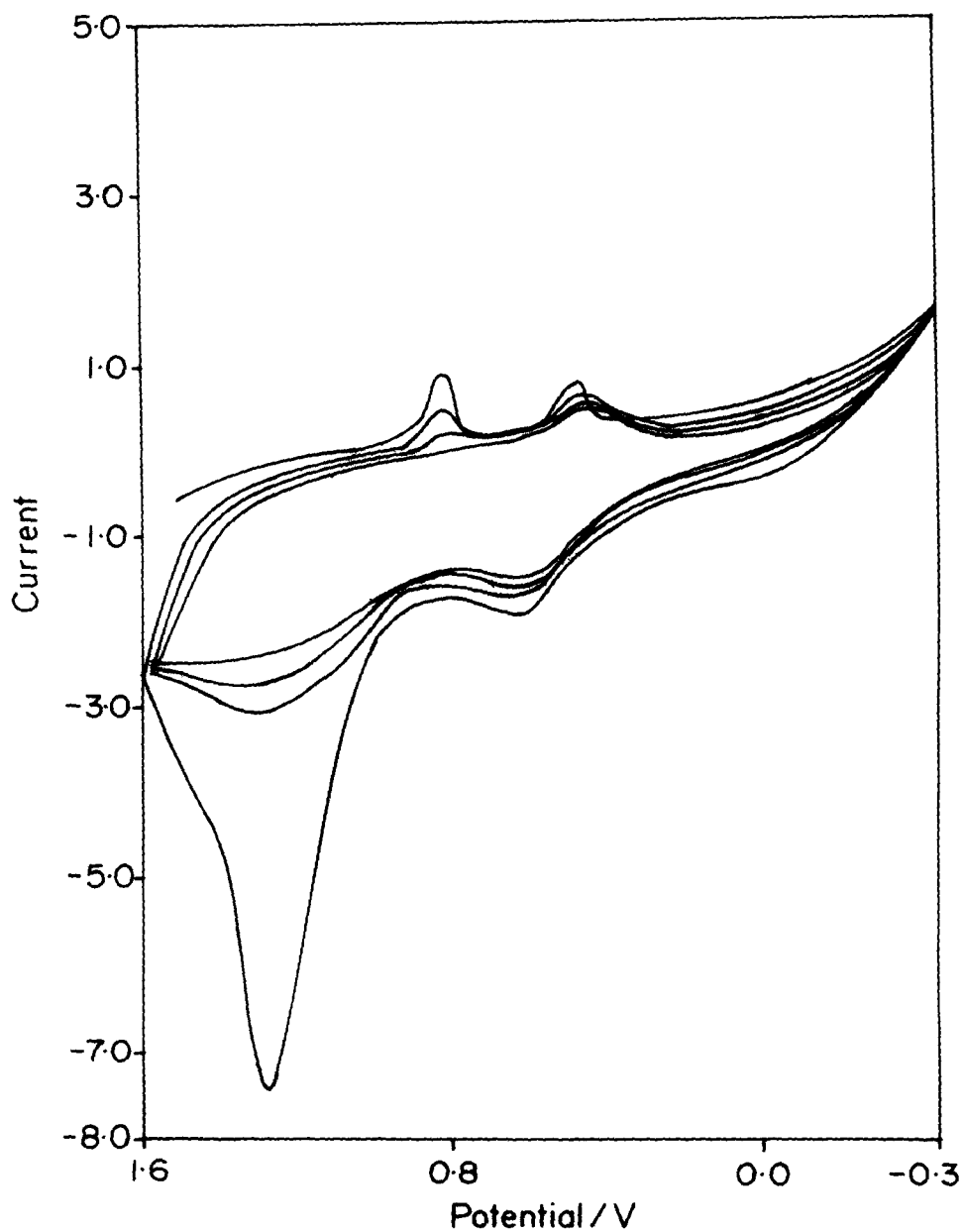


Fig. 3.4.2. Cyclic voltammogram of VO[T(*p*-OH)PP] in CH₂Cl₂ containing 0.1M TBAP at room temperature. Scan rate 0.05 V/s.

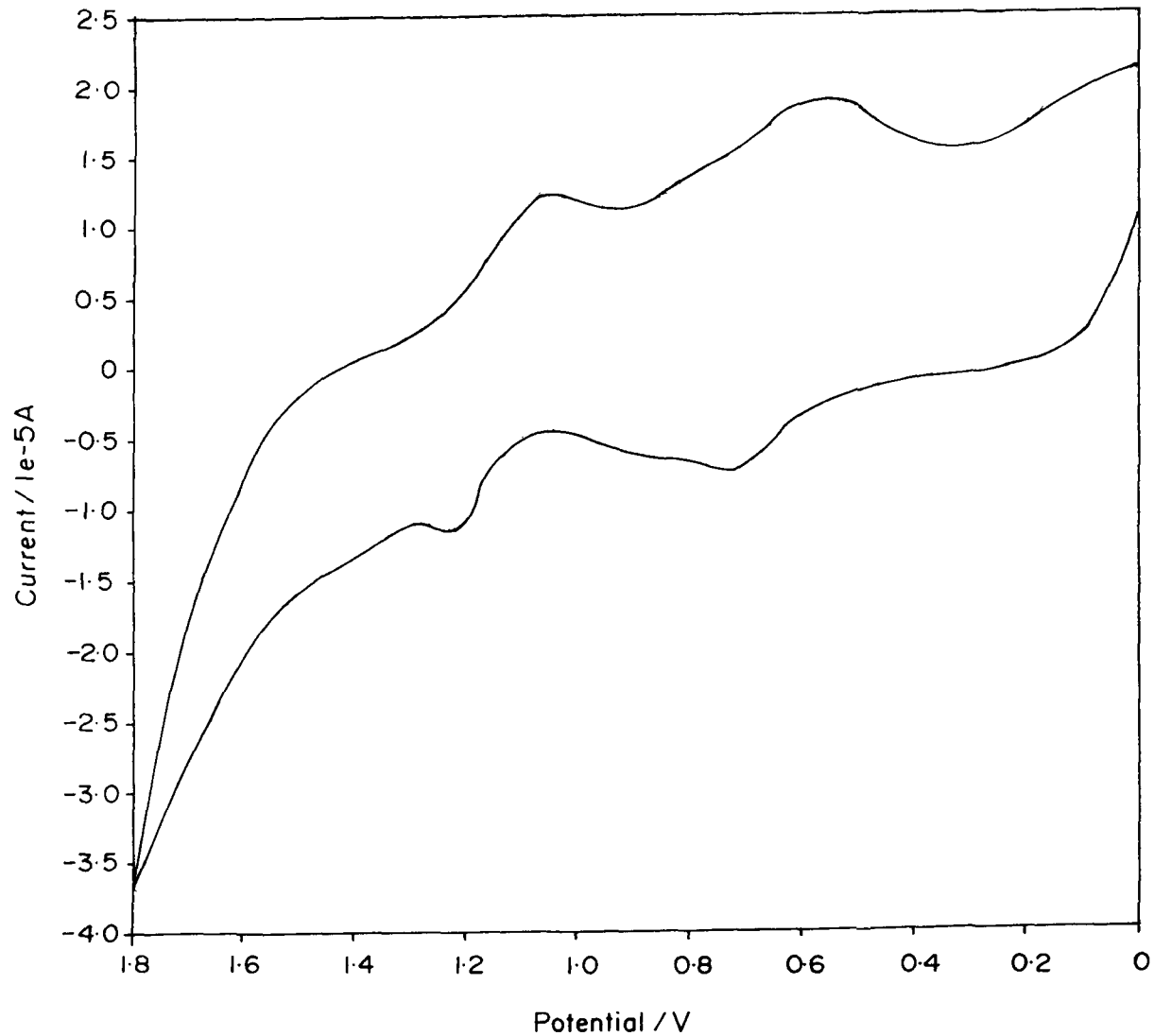


Fig. 3.4.3. Cyclic voltammogram of VO[T(*o*-NO₂)PP] in CH₂Cl₂ containing 0.1M TBAP at room temperature. Scan rate 0.1 V/s.

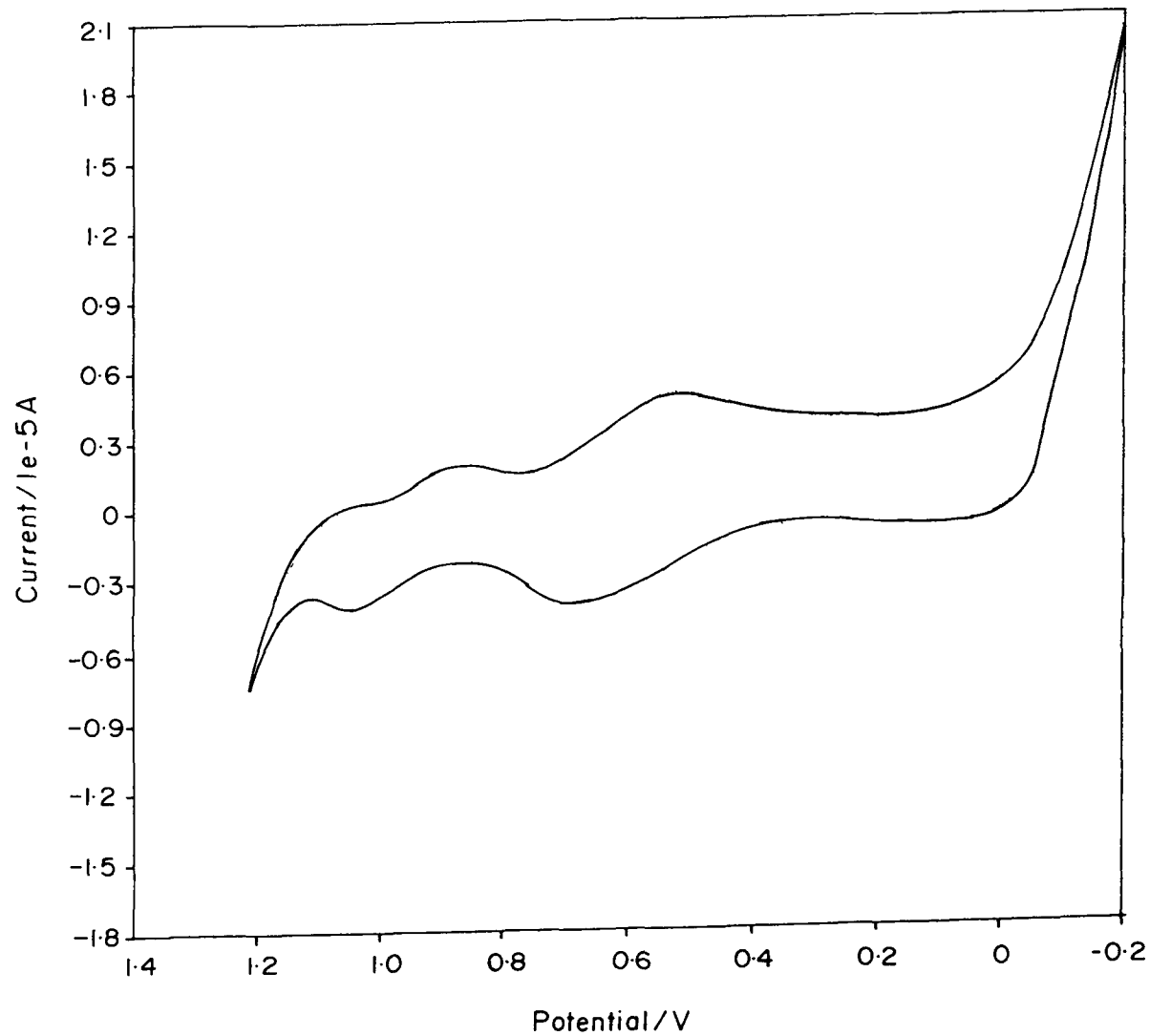


Fig. 3.4.4. Cyclic voltammogram of VO[TpyPP] in CH_2Cl_2 containing 0.1M TBAP at room temperature. Scan rate 0.01 V/s.

REFERENCES

1. R. H. Felton, in '*The Porphyrins*' edited by Dolphin(Academic press" , New York, 1979) **Vol.V**, p53 and references there in
2. D. G. Davies, In *The Porphyrins*" edited by Dolphin(Academic press" , New York, 1979) **Vol.V**, p127 and references there in
3. C. M. Newton and D. G. Davies, *J. Magn. Resonance.*, **20(4)**, 446(1975) and references there in
4. K. M. Kadish and M. Morrison, *Inorg. Chem.*,**15**, 930 (1976) and references there in
5. A. Girandean, H. J Callof and M. Gross, *Inorg. Chem.*, **18**, 201 (1979) and references there in
6. L. A. Bottomely, L. Olson, K. M. kadish, in "*Electrochemical and spectrochemical studies of Biological redox component*" Edited by K. M. Kadish (ACS advances, Washington,1982), p279 and references there in
7. R. Harada, H. Okawa and T. Kojima, *Inorg.Chim.Acta.*, **538**, 489 (2005) and references there in
8. I. Mayer, H. E. Toma, and K. Araki, *J. Elect.Ana. Chem.*, **590**,111(2006) and references there in
9. G. A. Mabboti, *J. Chem. Edn*, **60**, 697 (1983) and references there in

10. P. T. Kissinger and W. R. Heineman, *J. Chem. Edn.*, **60**, 702 (1983) and references there in
11. G. Canquis, V. D. Parker, in *"Organic Electrochemistry"* Edited by M. M. Baizer (Mancel Dekker, New York, 1973) p93 and references there in
12. *Operations Manual*, Bioanalytical System INC., West Lafayette, In, 1983 and references there in
13. G. Simonneaux, V. Schunemann, C. Morice, L. Carel, L. Toupet, H. Winkler, A. X. Trautwein, F. A. Walker., *J. Am. Chem. Soc.*, **122**, 4366 (2000) and references there in
14. A. Ghosh, I. Halvorsen, H. J. Nilsen, E. Steene, T. Wondimagegn, R. Lie, E. VanCaemelbecke, N. Guo, Z. Ou and K. M. Kaddish, *J. Phys. Chem. B*, **105**, 8120 (2001) and references there in
15. T. A. Evans, G. S. Srivatsa, D. T. Sawyer and T. G. Traylor, *Inorg. Chem.*, **24**, 4733 (1985) and references there in
16. A. Bettelheim, B. A. White, S. A. Raybuck and R. W. Murray., *Inorg. Chem.*, **26**, 1009 (1987) and references there in
17. A. Tomba Singh and A. Lemtur., *Spect. Chim. Acta., Part A.*, **59**, 1549 (2003) and references there in

CHAPTER 4

CYCLIC VOLTAMMETRIC STUDIES OF SOME MANGANESE, CADMIUM AND COPPER PORPHYRINS

4.1. INTRODUCTION

In Manganese porphyrins the central metal atoms as well as the ligand are electro active. Therefore, redox processes may occur in both the ligand as well as in the metal. Therefore, such systems give some interesting situation to study. Further, many workers have reported the catalytic activities of manganese porphyrins in alkane oxidations.

On the other hand cadmium and copper porphyrins do not have electro active metal center. Therefore, oxidation occurs in the ligand system. However, these oxidations depend on the central metal atom as well as the substitution in the ligand system. Further, redox processes will reflect the type of bonding that exists between the metal and the ligand¹⁻⁹.

4.2. RESULTS OF MANGANESE PORPHYRINS

Voltammograms of manganese porphyrins that are recorded are presented (fig.4.2.1, 4.2.2, 4.2.3 and 4.2.4). The results are summarized in the table 4.1. In all four manganese porphyrins three redox couples are observed.

Mn[T(2,5-(OCH₃)₂)PP] gives oxidation potentials 0.798V, 0.964V and 1.460V with their corresponding reduction potentials 0.5997V, 0.727V and 1.289V. Their ΔE values are 0.198V, 0.217V and 0.171V. Also $E_{1/2}$ values are 0.6989V, 0.8455V and 1.3745V.

Mn[T(*p*-OH)PP]: The oxidation potentials are 0.7255V, 1.1872V, and 1.2891V and their corresponding reduction potentials are 0.5675V, 0.8841V, and 1.1381V. ΔE values are 0.158V, 0.303V and 0.151V. Also $E_{1/2}$ Values are 0.6465V, 1.0357V, and 1.2136V.

Mn[T(*o*-NO₂)PP] : The oxidation potentials are 0.6493V, 0.9240V and 1.1988V and their corresponding reduction potentials are 0.5789V, 0.8404V, and 1.1188V. ΔE values are 0.0704V, 0.0836V and 0.08V. $E_{1/2}$ values are 0.6141V, 0.8822V and 1.1588V.

Mn[TpyP] : Oxidation potentials are 0.8521V, 1.2024V and 1.4902V with their corresponding reduction potentials 0.6408V and 1.5402V. ΔE values are 0.2113V and 0.050V and $E_{1/2}$ values are 0.7465 and 1.5152V.

4.3. DISCUSSION OF MANGANESE PORPHYRINS

The oxidation potential 0.798V of Mn[T(2,5-(OCH₃)₂)PP] is attributed to the oxidation of Mn(II)→Mn(III), while 0.964V and 1.460V are the first and the second ligand oxidations respectively. Irrespective of the large ΔE values, they exhibit reversibility (Fig.4.3.1, 4.3.2, 4.3.3 and 4.3.4)

For Mn[T(*p*-OH)PP], the oxidation potential 0.7255 V is attributed to Mn(II)→Mn(III) oxidation while 1.1872V and 1.2891V are the first and second ligand oxidations and are reversible. Another oxidation is observed at the potential 1.2891V without its counterpart reduction peak. This oxidation seems to be occurring at the ligand but not reversible. This could be due to polymerization at the electrode surface¹². It is also possible that due to polymerization oxidations potentials are observed to be at lower potentials compared to that of Mn[T(2,5-(OCH₃)₂)PP].

In Mn[T(*o*-NO₂)PP] the metal oxidation (Mn(II)→Mn(III)) occurs at 0.6493V while the ligand oxidations occur at 0.9240V and 1.1988V. We expected the oxidation potentials are to be shifted higher because -NO₂ is electron withdrawing group. Instead the potentials are shifted lower compared to Mn[T(2,5-(OCH₃)₂)PP]. On a possible reason could be due to ruffling in the porphyrin ligand structure¹⁰⁻¹³.

In the voltammogram of Mn[TpyP], three oxidations are observed with only two reduction peaks. The metal oxidation is observed at 0.8521V. Their E_{1/2} values are 0.050V and 0.746V. Only one redox couple for the ligand is observed. The oxidation potentials, are higher than that of Mn[T(o-NO₂)PP]. To understand these changes we need to investigate structural changes (porphyrin ligand ruffling) which are beyond the scope of this thesis.

4.4. CONCLUSION OF MANGANESE PORPHYRINS

From the CV studies of the above mentioned Manganese, porphyrins we confirm the following observations;

- i) In all four manganese porphyrins, Mn(II)→Mn(III) oxidation occurs although at slightly different potentials depending on the ligand.
- ii) Variation in the oxidation potential is attributed mainly to the nature of substitutions in the phenyl ring and the ruffling of the ligand structure.
- iii) In the case of Mn[T(*p*-OH)PP] polymerization at the surface of the electrode is observed.

4.5. RESULTS OF CADMIUM AND COPPER PORPHYRINS

Cd[T(2,5-(OCH₃)₂)PP] give two redox couples at E_{1/2} values 1.0486V and 1.2216V. Oxidation potentials are 1.0852V and 1.279V with their corresponding reduction potentials at 1.0120V and 1.1642 respectively. The ΔE values are 0.0732V and 0.1149V (fig, 4.5.1 and Table.4.2)

The voltammogram of Cd[T(o-NO₂)PP] show two oxidations at 0.7149V and 1.5324V with their corresponding reductions at 0.6027V and 0.9972V respectively. ΔE values are 0.1122V and 0.5352V and E_{1/2} values are 0.6588V and 1.2648V respectively (fig,4.5.2 and Table.4.2).

Cu[T(2,5-(OCH₃)₂)PP] voltammogram give two oxidations at 0.638V and 0.910V with their corresponding reductions at 0.5346V and 0.8098V respectively. The ΔE values are 0.1034V and 0.1002V and E_{1/2} values are 0.863V and 0.8599V (fig,4.5.3 and Table.4.2).

Cu[T(o-NO₂)PP] produces voltammogram consists of two oxidations at 0.7702V and 1.2145V with their corresponding reduction at 0.6607V and 1.0332V respectively. The ΔE values are 0.1095V and 0.1813V and E_{1/2} values are 0.7154V and 1.1238 (fig, 4.5.4 and Table.4.2)

4.6 DISCUSSION OF CADMIUM AND COPPER PORPHYRINS

For cadmium porphyrins two ligand oxidations are observed with their potentials higher than that of Cd(II)TPP. On the contrary Cd[T(o-NO₂)PP] exhibits lower oxidation potentials. This is quite surprising and we do not know why? Perhaps due to distortion in the ligand structure.

In the voltammogram of Cu[T(2,5-(OCH₃)₂)PP], the oxidation potentials are lower than that of Cu(II)TPP. This is as expected and is due to the electron donating group (-OCH₃). On the other hand the first oxidation potential of Cu[T(o-NO₂)PP] is lower than that of Cu(II)TPP while the second oxidation potential is slightly higher (Table.4.2). This is due to the electron withdrawing group (-NO₂) and the structural conformation of the porphyrin ligand¹⁰⁻¹³.

4.7. CONCLUSION OF CADMIUM AND COPPER PORPHYRINS

From the electrochemical studies of cadmium and copper porphyrins we observe the following;

- i) No redox processes occur at the metal center. The redox processes occur at the ligand.
- ii) Cu[T(2,5-(OCH₃)₂)PP] shows lowering in the oxidation potentials due to electron donating group(-

OCH₃). On the other hand Cu[T(o-NO₂)PP] show increase in the oxidation potentials due to the electron withdrawing group(-NO₂).

iii) Variations in the oxidation potentials may also be dependent on the ligand structural ruffling.

Table:4.1. Cyclic voltammetric data for manganese porphyrins at room temperature

Solvent: Dichloromethane

Supporting electrolyte: TBAP

Concentration : 10^{-3} M

Reference electrode : Ag/AgCl

System/	Scan Rate (V/s)	E _{pa} (1) V	E _{pa} (2) V	E _{pa} (3) V	E _{pc} (1) V	E _{pc} (2) V	E _{pc} (3) V	ΔE(1) V	ΔE(2) V	ΔE(3) V	E _{1/2} (1) V	E _{1/2} (2) V	E _{1/2} (3) V
Mn[T(2,5-(OCH ₃) ₂)PP]	0.1	0.798	0.964	1.460	0.5997	0.727	1.289	0.1983	0.217	0.1710	0.6989	0.8455	1.3745
Mn[T(p-OH)PP]	0.03	0.7255	1.1872	1.2891	0.5675	0.8841	1.1381	0.1580	0.3031	0.1510	0.6465	1.0357	1.2136
Mn[T(o-NO ₂)PP]	0.04	0.6493	0.9240	1.1988	0.5789	0.8404	1.1188	0.0704	0.0836	0.080	0.6141	0.8822	1.1588
Mn[TPyPP]	0.01	0.8521	1.2024	1.4902	0.6408	----	1.5402	0.2113	-----	0.050	0.7465	----	1.5152

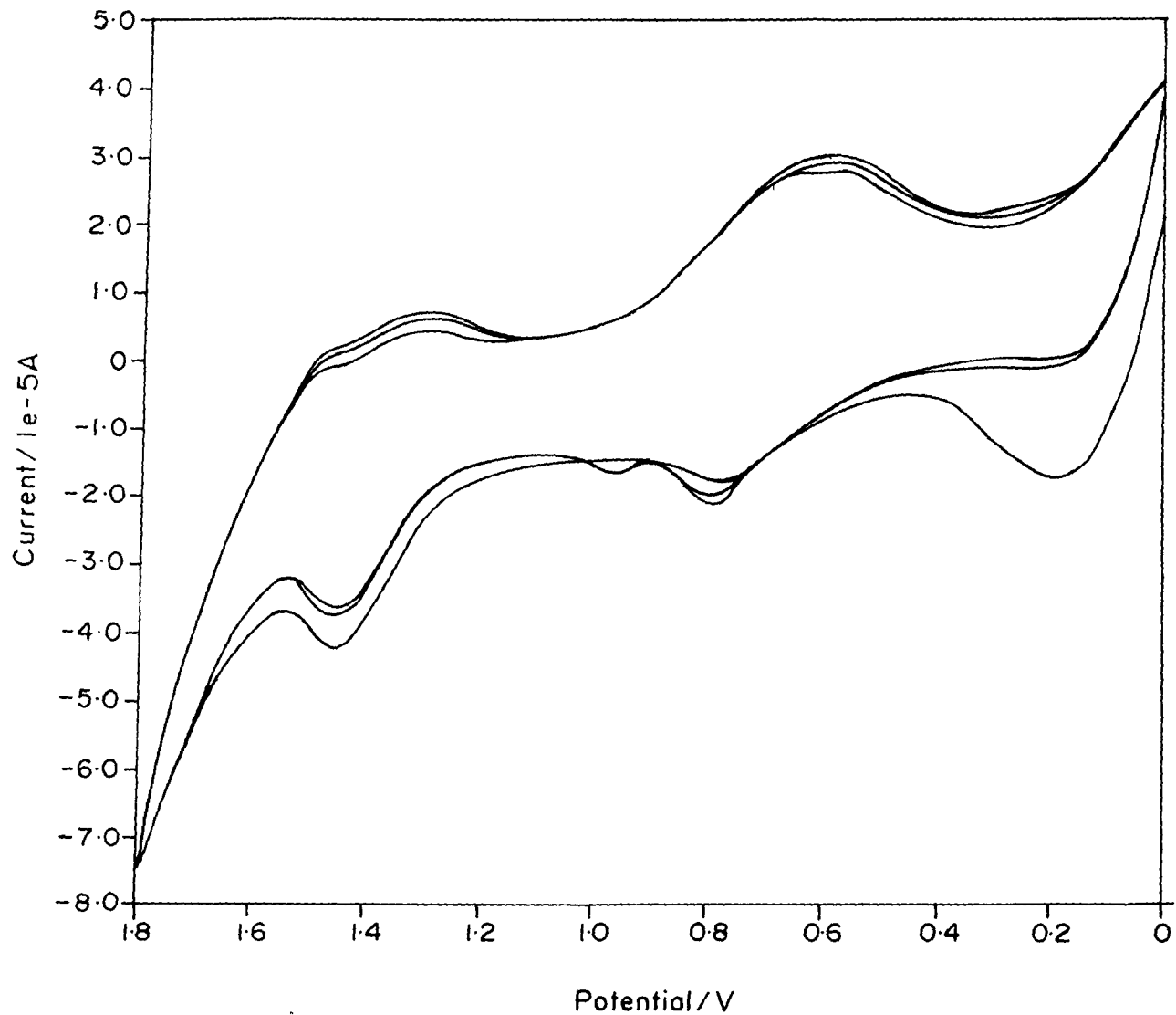


Fig.4.2.1. Cyclic voltammogram of $\text{Mn}[\text{T}(2,5\text{-(OCH}_3)_2\text{)PP}]$ in CH_2Cl_2 containing 0.1M TBAP at room temperature. Scan rate 0.1 V/s

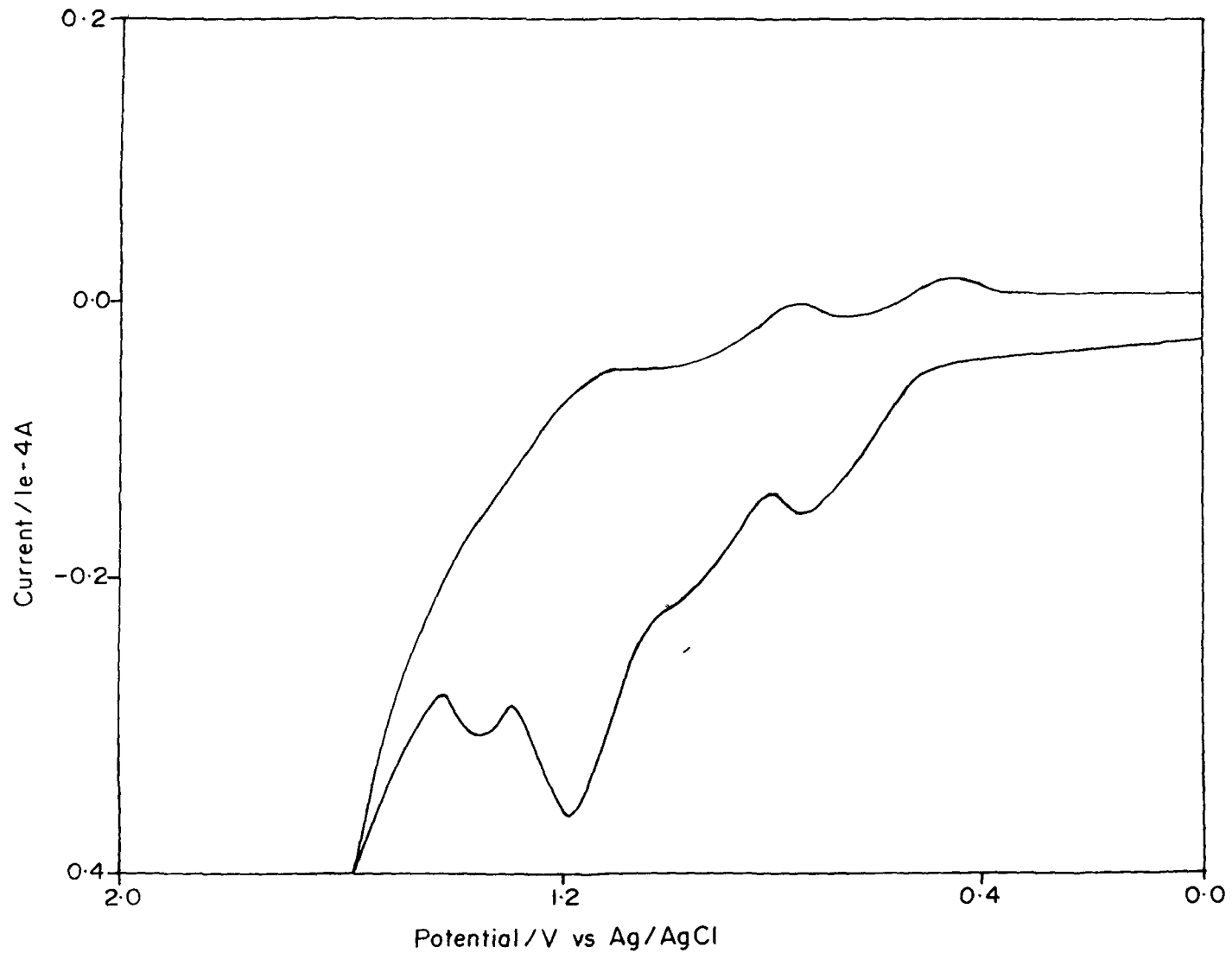


Fig.4.2.2. Cyclic voltammogram of Mn[T(*p*-OH)PP] in CH₂Cl₂ containing 0.1M TBAP at room temperature. Scan rate 0.03 V/s.

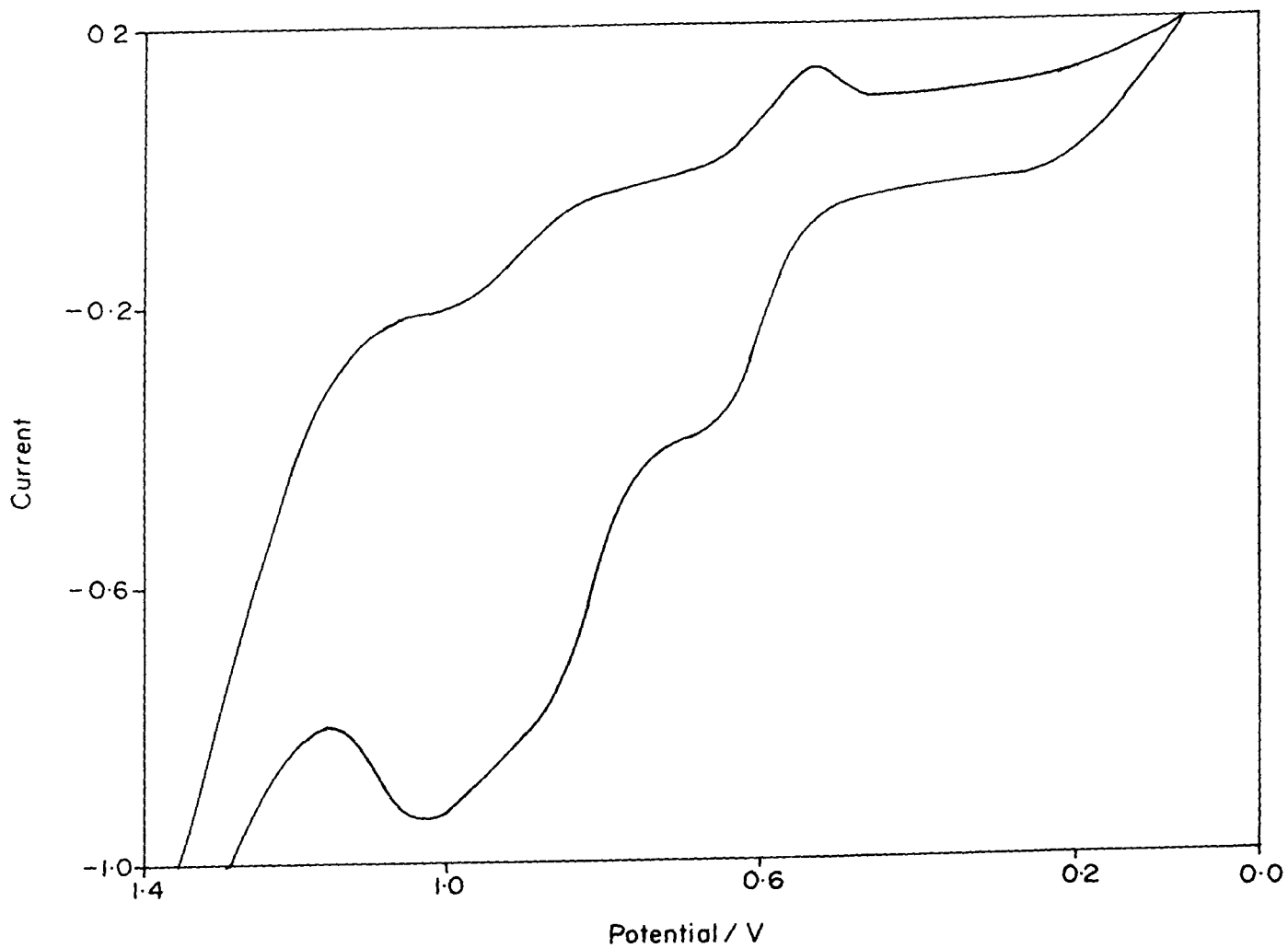


Fig.4.2.3. Cyclic voltammogram of Mn[T(*o*-NO₂)PP] in CH₂Cl₂ containing 0.1M TBAP at room temperature. Scan rate 0.04 V/s.

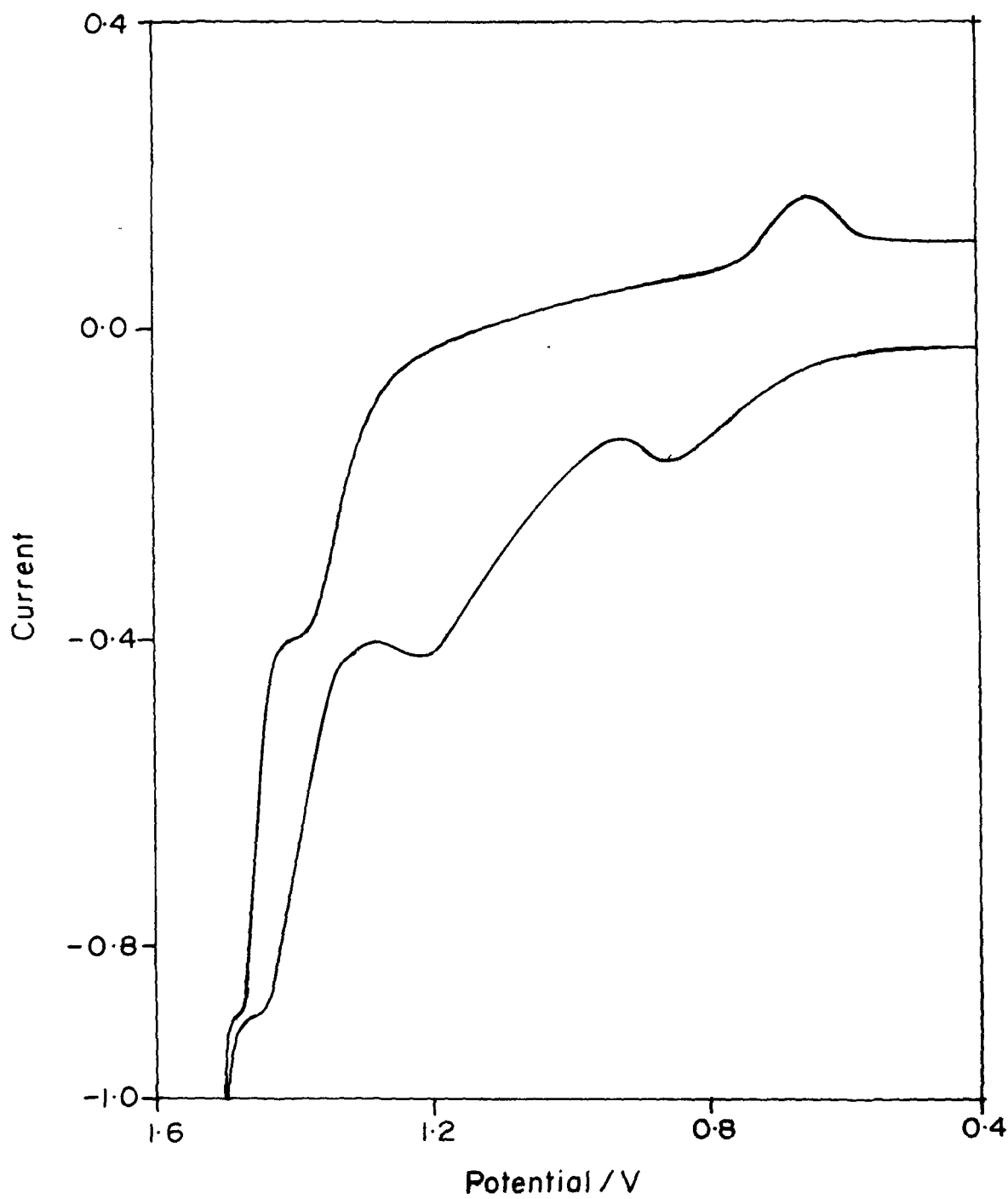


Fig.4.2.4. Cyclic voltammogram of Mn[TpyPP] in CH₂Cl₂ containing 0.1M TBAP at room temperature. Scan rate 0.01 V/s.

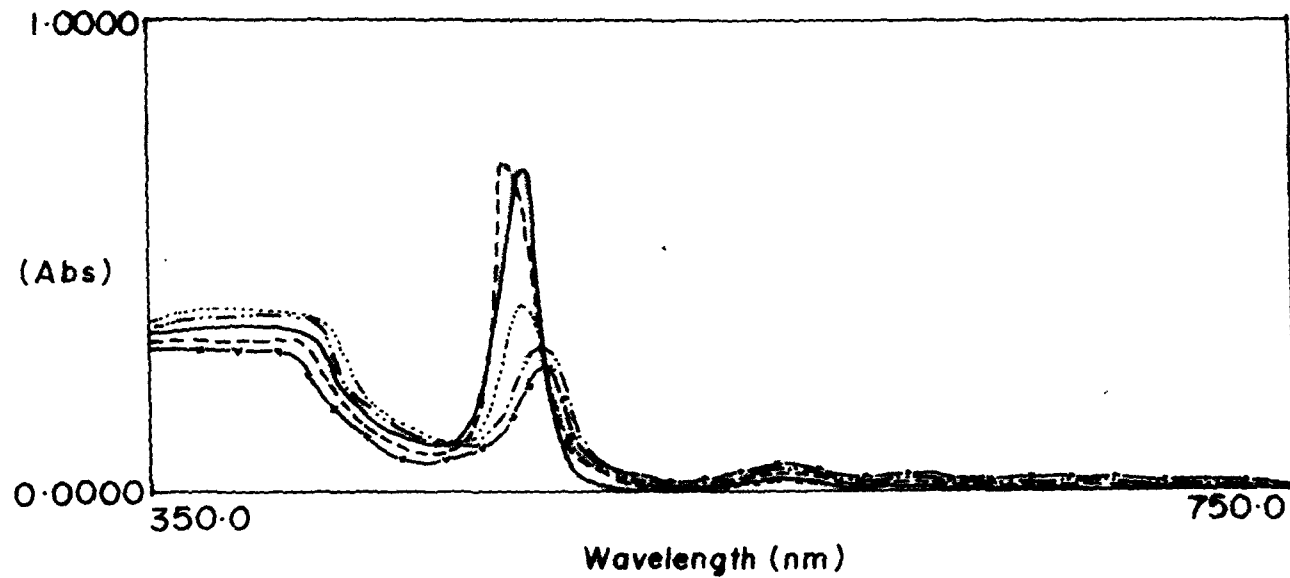


Figure.4.3.1..UV-visible absorption spectrum of $\text{Mn}[\text{T}(2,5\text{-(OCH}_3)_2\text{)PP}]$ in CH_2Cl_2 oxidized with (____) SbCl_5 at room temperature, (....), and (----) reduced with diethyl amine eth.

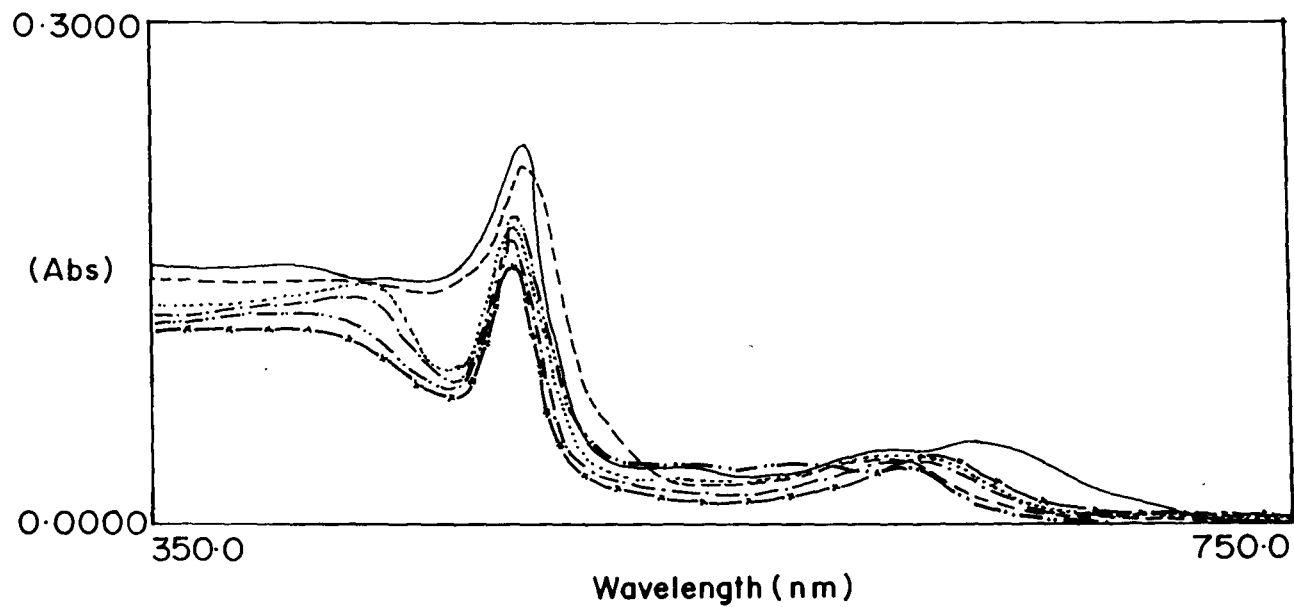


Figure.4.3.2..UV-visible absorption spectrum of Mn[T(p-OH)PP] in CH_2Cl_2 oxidized with (____) SbCl_5 at room temperature, (.....), ... and (—) reduced with diethyl amine

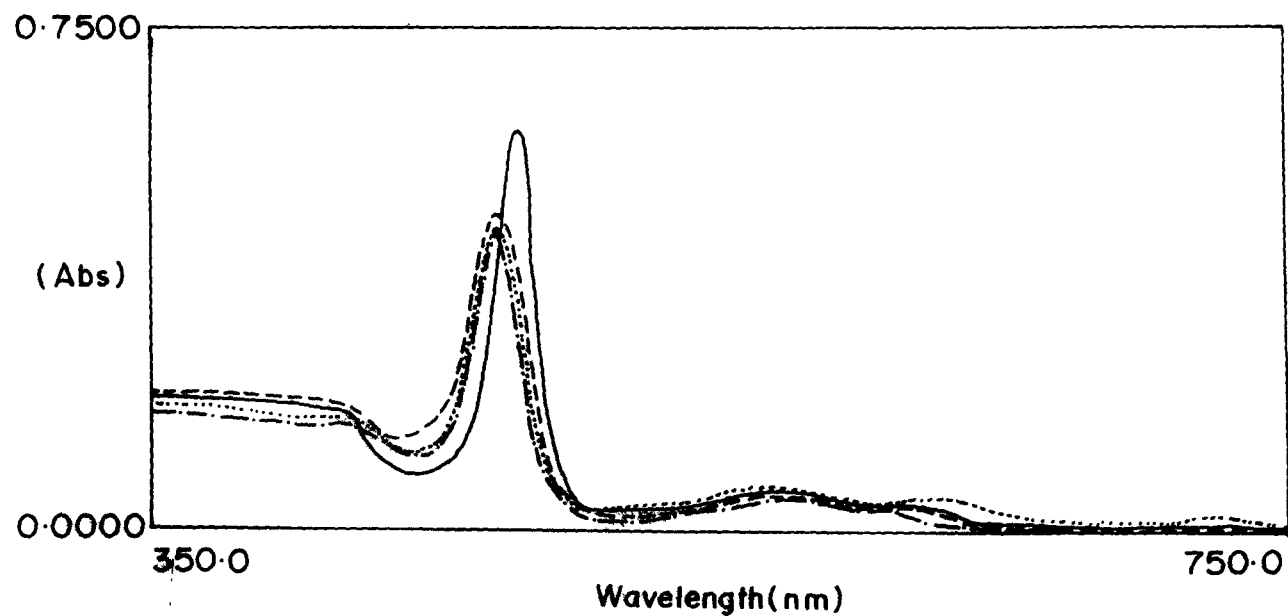


Figure.4.3.3..UV-visible absorption spectrum of Mn[T(*o*-NO₂)PP] in CH₂Cl₂ oxidized with(____)SbCl₅ at room temperature, (.....), and (----) reduced with diethyl amine

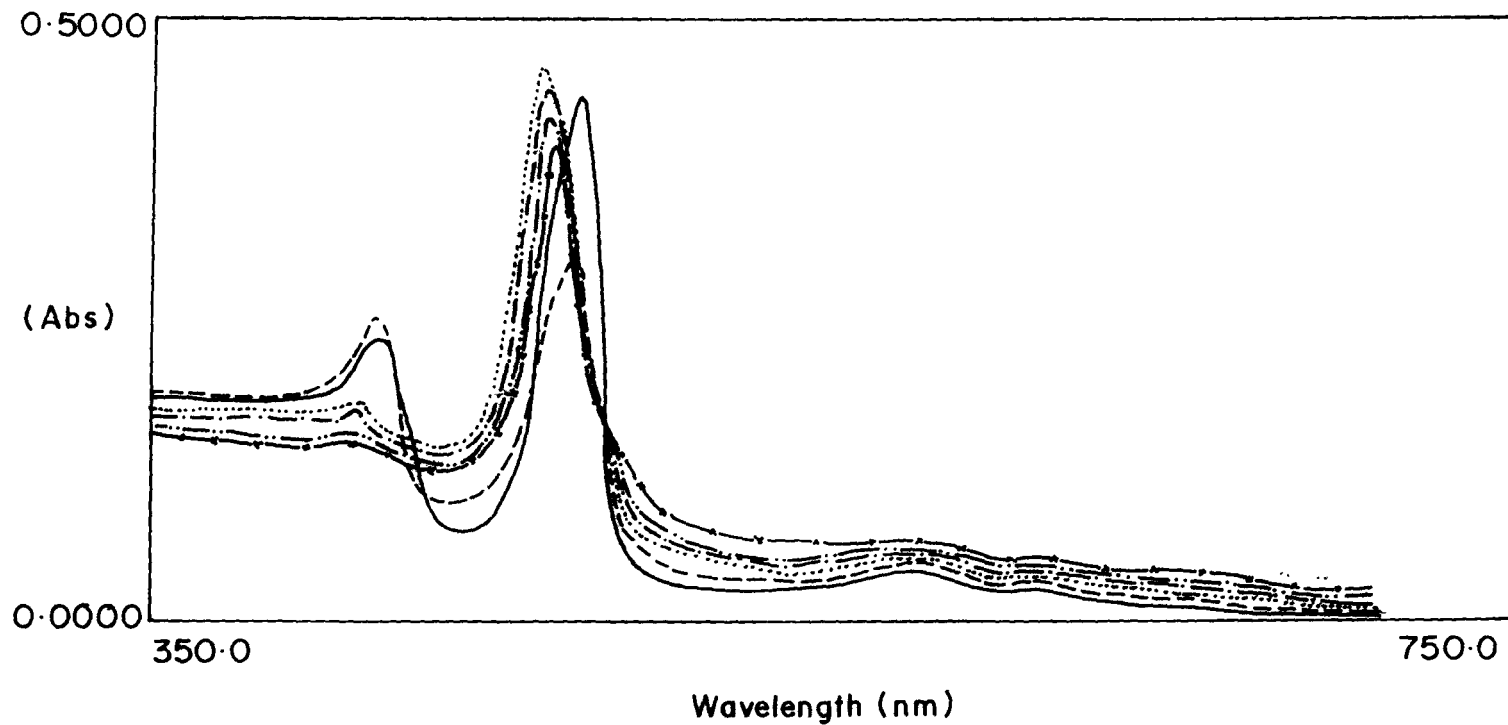


Figure.4.3.4. UV-visible absorption spectrum of Mn[TpyP] in CH_2Cl_2 oxidized with (____) SbCl_5 at room temperature, (....), and (----) reduced with diethyl amine

Table: 4.2. Cyclic voltammetric data for Cadmium and Copper porphyrins at room temperature

Solvent: Dichloromethane
 Supporting electrolyte: TBAP
 Concentration: $10^{-3}M$
 Reference electrode: Ag/AgCl

System/	Scan Rate (V/s)	Epa(1) V	Epa(2) V	Epa (3) V	Epc(1) V	Epc(2) V	Epc (3) V	$\Delta E(1)$ V	$\Delta E(2)$ V	$\Delta E(3)$ V	$E_{1/2}(1)$ V	$E_{1/2}(2)$ V	$E_{1/2}(3)$ V
Cd[T(2,5-(OCH ₃) ₂)PP]	0.06	1.0852	1.2791	----	1.012	1.1642	----	0.0732	0.1149	----	1.0486	1.2216	----
Cd[T(o-NO ₂)PP]	0.05	0.7149	1.5324	----	0.6027	0.9972	----	0.1122	0.5352	----	0.6588	1.2648	----
Cu[T(2,5-(OCH ₃) ₂)PP]	0.02	0.638	0.910	1.243	0.5346	0.8098	----	0.1034	0.1002	----	0.863	0.8599	---
Cu[T(o-NO ₂)PP]	0.05	0.7702	1.2145	----	0.6607	1.0332	----	0.1095	0.1813	----	0.7154	1.1238	----

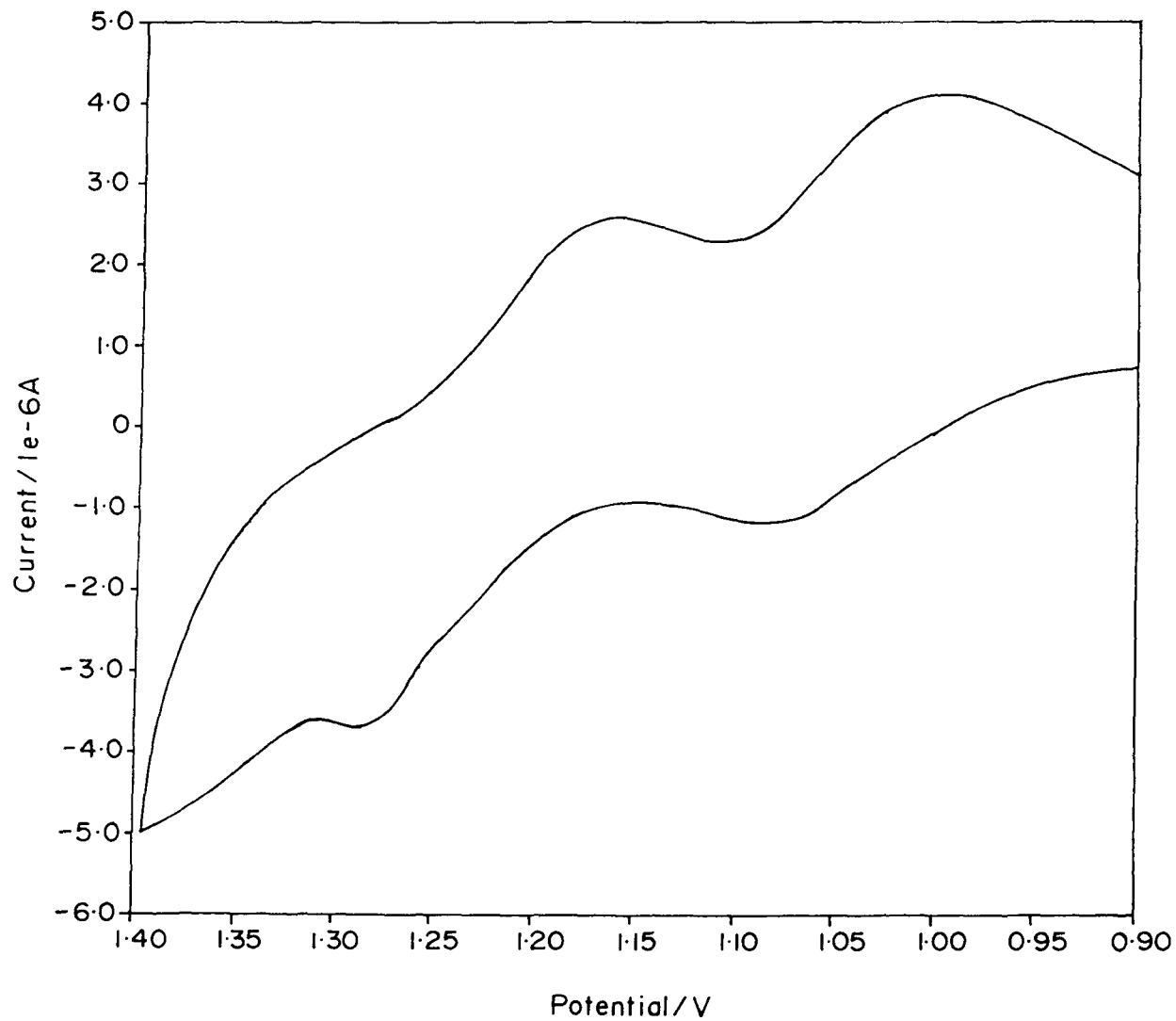


Fig.4.5.1. Cyclic voltammogram of Cd[T(2,5-(OCH₃)₂)PP] in CH₂Cl₂ containing 0.1M TBAP at room temperature Scan rate 0.06V/s

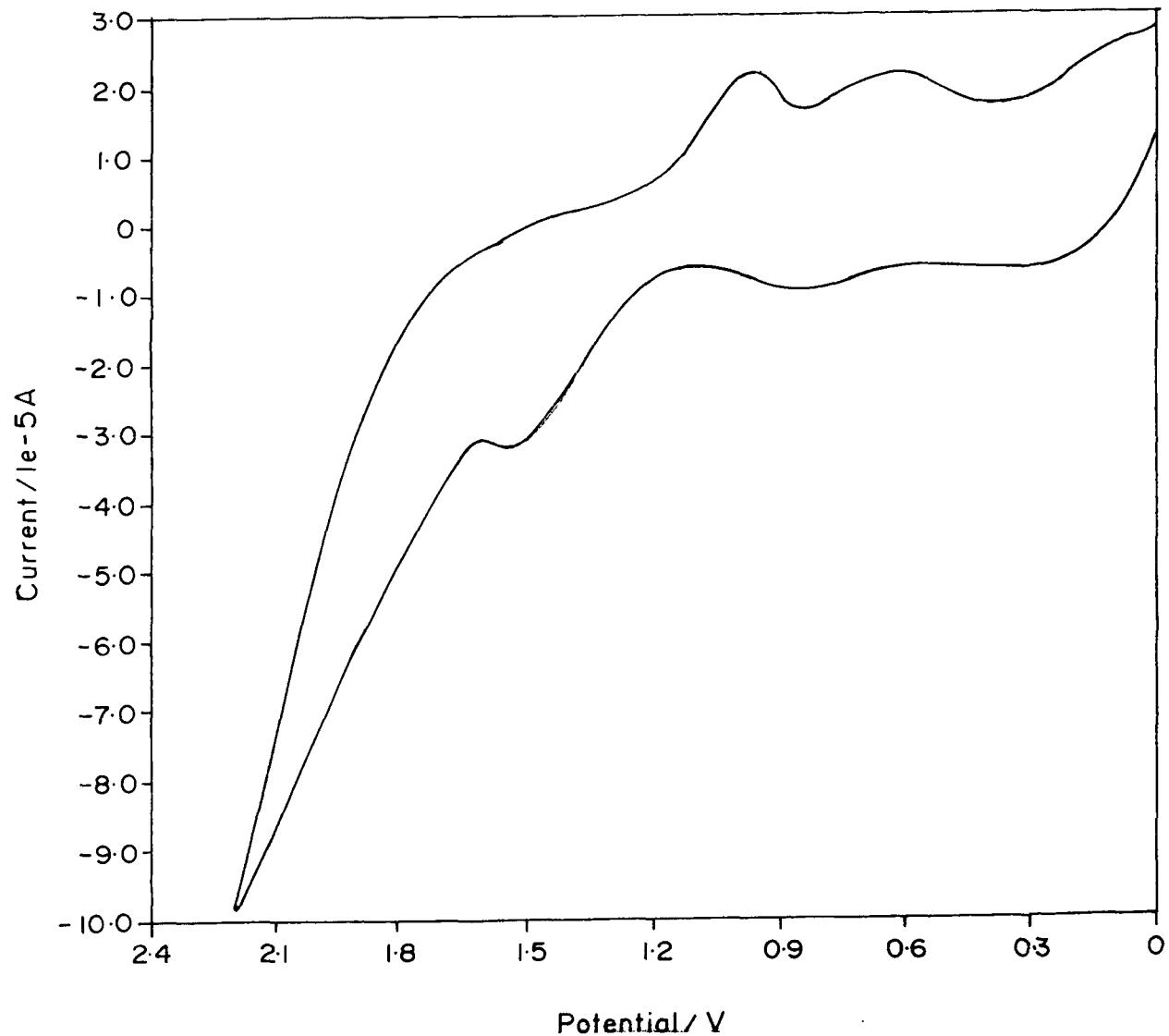


Fig.4.5.2. Cyclic voltammogram of Cd[T(*o*-NO₂)PP] in CH₂Cl₂ containing 0.1M TBAP at room temperature. Scan rate 0.05 V/s.

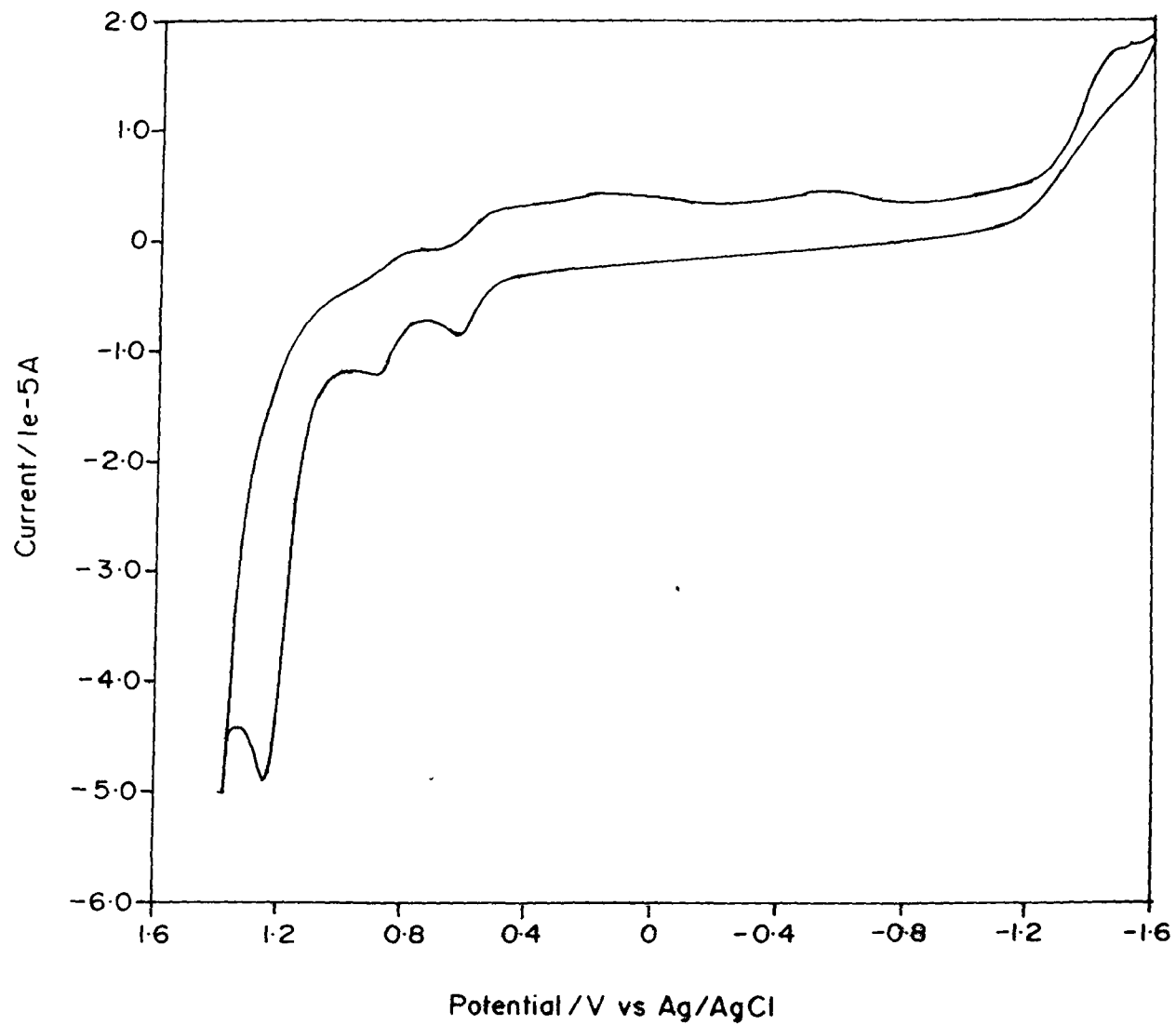


Fig.4.5.3. Cyclic voltammogram of Cu[T(2,5-(OCH₃)₂)PP] in CH₂Cl₂ containing 0.1M TBAP at room temperature. Scan rate 0.02 V/s

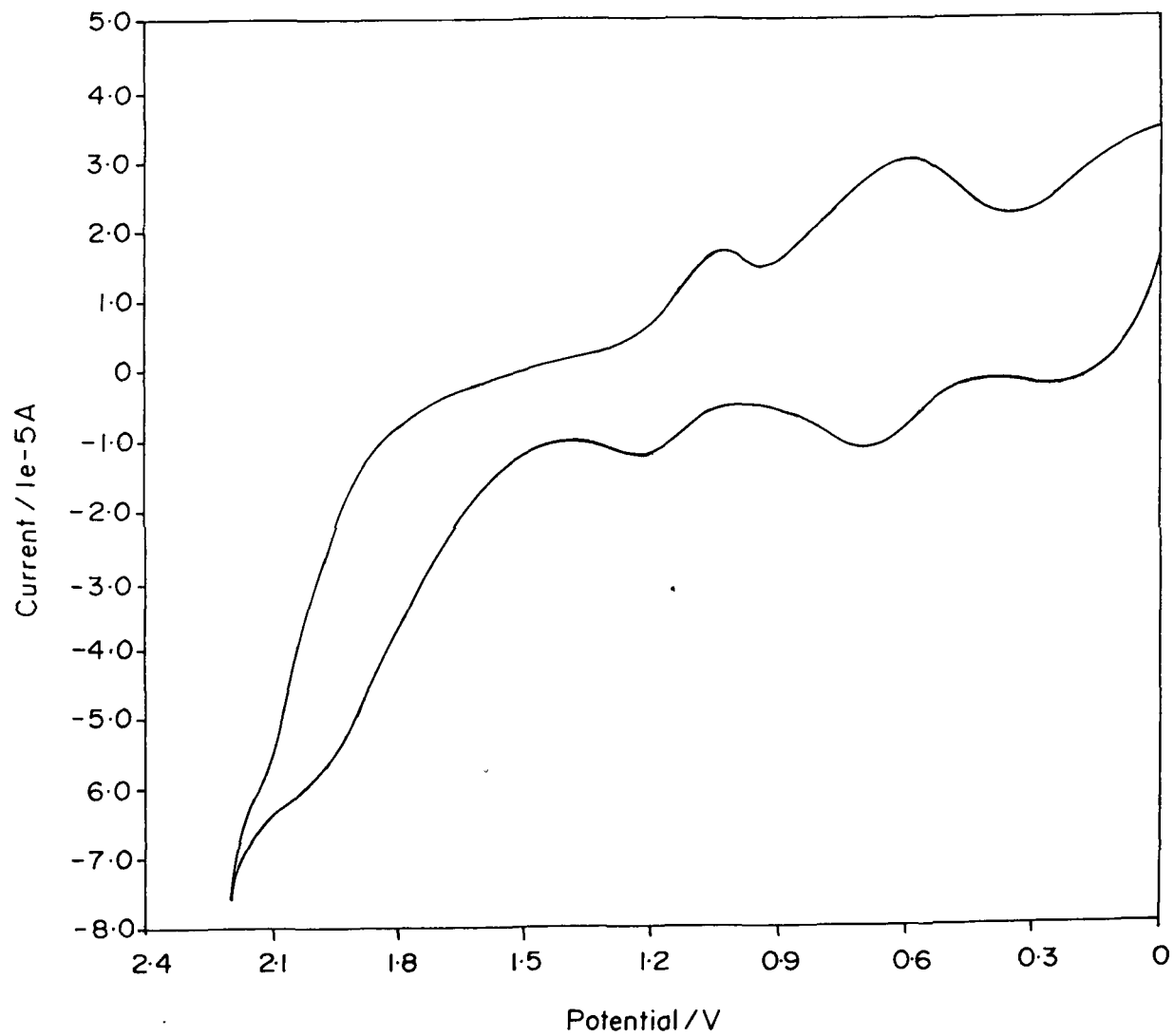


Fig.4.5.4. Cyclic voltammogram of Cu[T(*o*-NO₂)PP] in CH₂Cl₂ containing 0.1M TBAP at room temperature. Scan rate 0.05 V/s.

REFERENCES

1. C. L. Hill and B. C. Schardt, *J. Am. Chem. Soc.*, **102**, 6375 (1980) and references there in
2. J. T. Groves, W. J. Kruper, and R. C. Haushalter., *J. Am. Chem. Soc.*, **102**, 6377, (1980)and references there in
3. B. C. Schardt, F. T. Hoolander and C. L. Hill., *J. Am. Chem. Soc.*, **104**, 3964 (1982) and references there in
4. C. L. Hill and J. A. Smegal, *New. J. Chem.*, **6**, 287 (1982) and references there in
5. J. A. Smegal, B. C. Schardt, and C. L. Hill, *J. Am. Chem. Soc.*, **105**, 3510 (1983) and references there in
6. J. A. Smegal and C. L. Hill, *J. Am. Chem. Soc.*, **105**, 3515 (1983) and references there in
7. J. T. Groves and M. K. Stern., *J. Am. Chem. Soc.*, **110**, 8628 (1988) and references there in
8. G. R. Friederman, M. Halma, K. D. de F. Castro, F. L. Bedito, F. G. Doro, S. M. Drechsel, A. S. Mangrich, M. D. D. Assis and S. Nakagaki., *Applied Cata.A Gen.*,**308**, 172 (2006) and references there in
9. D. M. Gold, M. Kumar and P. Neta, *J. Phys. Chem.*, **96**, 9576 (1992) and references there in

10. G. Simonneaux, V. Schunemann, C. Morice, L. Carel, L. Toupet, H. Winkler, A. X. Trautwein, F. A. Walker., *J. Am. Chem. Soc.*, **122**, 4366 (2000) and references there in
11. A. Ghosh, I. Halvorsen, H. J. Nilsen, E. Steene, T. Wondimagegn, R. Lie, E. VanCaemelbecke, N. Guo, Z. Ou and K. M. Kaddish, *J. Phys. Chem.B*, **105**, 8120(2001) and references there in
12. A. Bettelheim, B. A. White, S. A. Raybuck and R. W. Murray., *Inorg.Chem.*, **26**, 1009(1987) and references there in
13. R. Harada, H. Okawa and T. Kojima, *Inorg.Chim.Acta.*, **538**, 489 (2005) and references there in

CHAPTER 5

ESR OF SOME SUBSTITUTED VANADYL MESO-TETRAPHENYL PORPHYRINS OXIDIZED WITH $SbCl_5$

5.1. INTRODUCTION

Electron paramagnetic resonance (EPR) is a technique which is extensively used by chemists and other scientists to monitor the paramagnetic properties of the system they study. The basic theories of the EPR are well documented in the literature. In porphyrin chemistry EPR has been used extensively and exhaustive literatures are available. In view of this we simply present here a very brief and selective discussion on paramagnetic resonance theory

In a metalloporphyrin one or more unpaired electrons may exist on the central metal atom. Also one or more unpaired electrons may be generated on the π -ligand system or on the central metal atom or in both. Such unpaired electrons will give paramagnetic signal and will give rise to EPR spectra. The features of EPR spectra are dependent on the number of unpaired electrons and its environment.

5.2. SOME BASIC PRINCIPLES OF ESR¹⁻⁷

5.2.1. Resonance Condition, g-value and symmetry

An unpaired electron is associated with a spin angular momentum giving rise to a magnetic moment μ , which is given by

$$\mu_e = g\beta_s \dots \dots \dots (4.2.1)$$

Where g is the electron g factor and is dimensionless. β is the electronic Bohr magneton ($=e\hbar/2mc$, where $e = -e$, charge on the electron and $m =$ mass of the electron).

If we subject such a system to an external magnetic field \mathbf{B} , the interaction between the electron magnetic moment and the external magnetic field is given by the Hamiltonian

$$\mathbf{H} = - \mu \cdot \mathbf{B} \dots \dots \dots (4.2.2)$$

From equations (4.2.1) and (4.2.2), we get

$$\mathbf{H} = g\beta_e \mathbf{B} \cdot \mathbf{S} \dots \dots \dots (4.2.3)$$

If the applied magnetic field is in the Z-direction, then

$$\mathbf{H} = g\beta_e B_z S_z \text{ -----} (4.2.4)$$

Since $S_z = \pm 1/2$, we can have two allowed orientations of spins ($M_s = \pm 1/2$) parallel or antiparallel to H_z , Replacing the Hamiltonian H by E (Energy), then equation (4.2.4) can be written as

$$E = (\pm 1/2) g\beta_e B_z \dots \dots \dots (4.2.5)$$

Since $\Delta E = h\nu \dots \dots \dots (4.2.5)$

We get

$$h\nu = g\beta_e B_z \dots\dots\dots(4.2.7)$$

gives the resonance condition. The frequency of electromagnetic radiation required to induce transitions between the two spin states is given by

$$\nu = (g\beta_e/h) B_z \dots\dots\dots(4.2.8)$$

For a magnetic field of 3500G, the absorption frequency lies in the X-band (3 cm) microwave region. The selection rule for an EPR transition is $\Delta M_s = \pm 1$, with the irradiation oscillating magnetic field being perpendicular to the external magnetic field.

One can determine the g-value, from the experimental EPR spectrum. It's value is mainly dependent on the spin and the orbital angular momentum of the unpaired electron. For a spherically symmetric system(S-state) the orbital angular momentum is zero and the g-value is more or less equal to free-spin value $g = 2.0023$. For an organic free radical, the electrons are delocalized, and have very little angular momentum resulting in a small derivation from the free electron g-value. The picture is different in the case of transition metals. In a transition metal complex the orbital angular momentum of the metal electron(s) is quenched fully or partially by the ligand atoms or by other neighboring ions. This leads to a deviation from the free spin g-value.

This correlated to the spin-orbit interactions. In solid state g-value depends on the symmetry i.e. the orientation of the magnetic field to the symmetry axes of the electric field about the ion. This leads to the anisotropy in g-values. One can observe EPR signals at two g-values for a polycrystalline sample if the ligand field has an axial symmetry. For such system two types of absorptions are exhibited in the spectrum. A major absorption is observed if the external magnetic field is perpendicular to the symmetry axis (considering the symmetry axis as Z axis, then $g_x = g_y = g_{\perp}$) and minor absorption is observed if the applied field is parallel to the symmetry axis. Most of the metalloporphyrins have axial symmetry and we observe two g-values. If the symmetry changes, we may observe more g-values. This is what we observe in the case of orthorhombic, where three different g-values are exhibited. On the other hand the situation is different in solution. The molecules are in rapid tumbling motion and averages out to a single g-value. It is also to be noted that the g-value depends on the oxidation state of the metal ion.

5.2.3. ZEROFIELD SPLITTING AND FINE STRUCTURE

For a system having a total spin $S > 1/2$ i.e. having more than one unpaired electron, we often see some $2S$ features in the spectra especially in the oriented system. This structure is known as fine structure. This fine structure is due to the interaction of the individual magnetic moments (due to spin) with the magnetic fields generated by other electrons. This interaction exists even in the absence of the external magnetic field. This phenomenon is called the zero field splitting. Thus, the fine structure reflects a splitting of the $(2S+1)$ levels in the absence of the external magnetic field. Obviously, zero field splitting lead $\Delta M_S = 1$ transitions to occur at different values of the applied field for a particular microwave frequency. The EPR spectrum of $\Delta M_S = 1$ transitions is sometimes anisotropic and one can determine the zero field splitting from its analysis. Zero field splitting observed for transition metal ions if there are some distortions in the cubic symmetry. The effect of zero field splitting for $\Delta M_S = 1$ and $\Delta M_S = 3/2$ is shown below (fig.5.2.1) . From the EPR measurements of the zero field splitting one can also approximately calculate the average distance between two unpaired electrons of a triplet state (organic triplet state molecule).

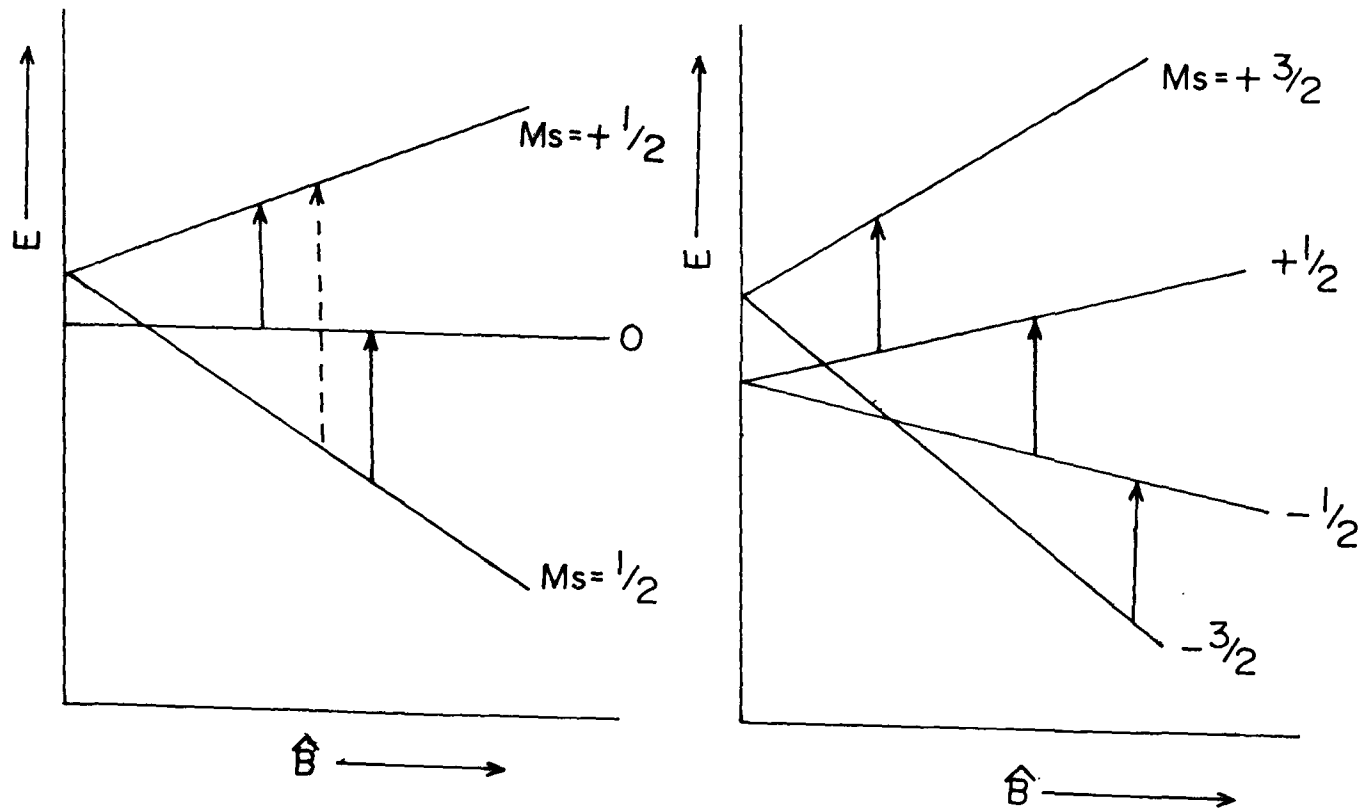


Fig.5.2.1. Effect of zero field splitting, Energy levels
 A triplet state (ii) a quartet state for of an axially symmetric system
 Arrow (\rightarrow) indicates $\Delta M_s = 1$ and dotted line ($\cdots\rightarrow$) indicates $\Delta M_s = 2$

5.3. HYPERFINE INTERACTION

One of the main objectives of the EPR measurements is to obtain the hyperfine splittings, and to analyze and interpret it. The hyperfine interactions originate from the interaction between the magnetic moment of the unpaired electron spin and the magnetic moment of the nuclei present in the system. There are two types of such interaction viz. (a) Fermi contact interaction and (b) Dipolar interaction.

(a) FERMI CONTACT INTERACTION

This interaction occurs due to the non vanishing electron spin density on the surface of the nucleus or in the S-orbital of the atom. This is so because p, d, f orbitals have nodes at the nucleus. In the case of the organic π -radical the hyperfine interaction of occurs due to $\sigma -\pi$ spin polarization mechanism. Similarly, a contact interaction occurs involving a transition metal ion. In both cases some electron spin density should exist in the S-orbital of the atom. This spin polarization mechanism is explained elsewhere in the literature. However, the better explanation may be given if we invoke Realistic quantum mechanics. The hyperfine coupling constants are observed to be much large for transition metal ions than those for organic free radicals.

(b) THE DIPOLAR INTERACTION

This interaction is similar to the classical dipolar interaction between two bar magnets. In solution this interaction averages out to zero due to rapid tumbling motions of the molecules. We normally observe this interaction only in the solid state. Therefore, it depends on the orientation of both the magnetic moments i.e. Electron spin moment and the nuclear magnetic moment with respect to the applied magnetic moment. Thus, it is anisotropic. This interaction becomes more complicated in the case of transition metal ion due to spin-orbit coupling which is also dependent on the symmetry of the molecule.

5.4. LINE SHAPE AND RELAXATION

To obtain information out of EPR spectra one has to study the line shape /line widths. Shape of the EPR lines depends greatly on the spin relaxation time. We observe EPR absorption line due to population difference between the two spin states (large population in the lower energy spin state) at thermal equilibrium. This condition is maintained by spin relaxation. Therefore, it is obvious that the spin states have finite life time. Thus, the line widths of an EPR spectrum are inversely proportional to the relaxation time. In this case the relaxation

undergo without emission of radiation. The relaxation process through two mechanisms via spin-lattice relaxation and spin-spin relaxation. Spin-lattice relaxation involves spin-orbit coupling. Strong spin-orbit coupling results in a short spin-lattice relaxation time (T_1) giving broad lines or sometimes too broad for detection (say at room temperature). On lowering the temperature (liquid nitrogen, liquid helium) the spin lattice relaxation time (T_1) increases and we observe EPR spectra. Obviously, at lower temperature the lower energy spin state population increases and we observe better EPR spectra. One observes sharper EPR spectra for free radicals even at room temperature. This is because in free radicals, the spin-orbit coupling is negligible and gives rise to longer spin-lattice relaxation time. Thus, free radicals exhibit narrower line widths

Spin-spin relaxation occurs due to the intermolecular interactions. A particular molecule having an unpaired electron will have spin moment which will be affected by the local field generated by the neighboring spins. These local fields produce fluctuation in the actual external magnetic applied (B_0). Therefore, this particular spin will experience a field equal to $B_0 + B_{\text{local}}$. Further, it also induces transitions within the system. Obviously, spin-spin relaxation is concentration dependant. Thus, spin-spin

relaxation time (T_2) decreases with increase in concentration and vice versa. Therefore, for a strong paramagnetic sample, sharper EPR lines will be obtained on dilution.

Besides, these two processes mentioned above there are other factors that contribute to the EPR line shape.

Normally, one encounters of line shapes via, Lorentzian and Gaussian. In solution spectra one commonly encounters Lorentzian line shape, which is given by

$$f(w) = [(1/\hbar)(1/T_2)] / [(1/T_2)^2 / (w_0 - w)]^2 \dots\dots\dots (4.4.1)$$

In solid spectra one generally observe Gaussian line shape which is given by

$$f(w) = T_2(2\hbar)^{-1/2} \exp[-1/2 T_2^2(w_0-w)^2] \dots\dots\dots (4.4.2)$$

5.5. SPIN HAMILTONIAN

One can write the spin Hamiltonian for Hydrogen atom easily as

$$H = g\beta BS_z - g_N\beta_N B I_z + a.S.I \dots\dots\dots(4.5.1)$$

The third term in the equation (4.5.1) tells that it is isotropic hyperfine coupling, but does not indicate anything about the mechanism of the coupling. Therefore, one has to formulate proper spin Hamiltonian and obtain the values of these parameters from the experimental EPR spectra and fit them into the spin Hamiltonian. In transition metal ions, spin-orbit coupling

complicates the EPR spectra. In the spin Hamiltonian terms like **S.B**, **L.B**, **S.I.S.I**, **L.I**, **S.L** and **S₁.S₂** occur.(where **S** = electron spin, **I** = nuclear spin **B**= external magnetic field, **L** = orbital angular momentum and **S₁** and **S₂** are the spins electrons 1 and 2 respectively). To interpret the EPR spectra in terms of these interactions is quite different and not straightforward. The effect of the spin-orbit coupling is included in the g-values ($g_x = g_y = g_z$) and the hyperfine coupling A_x , A_y , A_z . These values can be obtained from the experimental EPR spectra and then fit into the spin Hamiltonian. One can compute the spin Hamiltonian parameters by proper choice of wave function. It is to be noted that the Hamiltonian has to be defined with respect to the co-ordinates of g tensor and A tensor in which they are diagonal.

5.6. METALLOPORPHYRINS WITH PARAMAGNETIC METAL ATOM UNPAIRED ELECTRON ON THE LIGAND

In general there are two types of porphyrin ligands: (i) OEP-type (OEP = octa ethyl porphyrin) and (ii) TPP type (TPP = meso tetraphenyl porphyrin)⁸⁻¹³.

- (i) OEP type: The porphyrin ligands which do not have any substituents in the meso positions. Typical examples

are octaethyl porphyrin, Etio porphyrin, proto porphyrin and many other naturally occurring porphyrins.

- (ii) TPP type: The porphyrin ligands which have alky or aryl substituents into meso positions. Typical example is mesotetraphenyl porphyrin. etc.

In a metalloporphyrin having D_{4h} symmetry, the highest occupied pi molecular orbits are very close lying, with symmetry labels a_{1u} and a_{2u} . The energy difference between these two molecular orbitals is of the order of 0.5ev or less. Therefore, their relative ordering is quite sensitive to the central metal ion. However, it has been normally observed that for metalloporphyrin radical cations belonging to OEP type the HOMO (Highest occupied molecular orbital) have a_{1u} ground state. On the other hand that of the TPP type has a_{2u} ground state. It is to be noted that these generalization is not rigid and in some case the ground state of the pi radical changes from a_{1u} to a_{2u} on changing the axial ligand. On the whole the above generalization holds fairly well for a large number of metalloporphyrin,

5.7. ESR OF SOME SUBSTITUTED VANADYL meso-TETRAPHENYL PORPHYRINS OXIDIZED WITH SbCl₅

5.7.1. RESULTS

(I) VO[T(*o*-NO₂)PP]

Oxidation of VO[T(*o*-NO₂)PP] with SbCl₅ follows exactly in the same manner to that of the VOTPP oxidation. Addition of 1.8ml of 0.1M SbCl₅ to 0.2ml of 10⁻³M VO[T(*o*-NO₂)PP] gives rise to the spectrum(fig.5.7.1(i)). Further addition of SbCl₅ leads to triplet state.

(II) VO[T(2,5-(OCH₃)₂)PP]

Addition of 2.6ml of 0.1M SbCl₅ to 0.2ml of 10⁻³M VO[T(2,5-(OCH₃)₂)PP] give the spectrum(fig.5.7.1(ii)A). Further addition of SbCl₅ leads to triplet (fig.5.7.1(ii)B). This leads to a triplet state.

(III) VO[TpyP]

Addition of 1.2ml of 0.1M SbCl₅ to 0.2ml of 10⁻³M VO[TpyP] exhibits the spectrum(fig.5.7.1(iii)A). Further addition of SbCl₅ yield the spectrum (fig.5.7.1(iii)B).

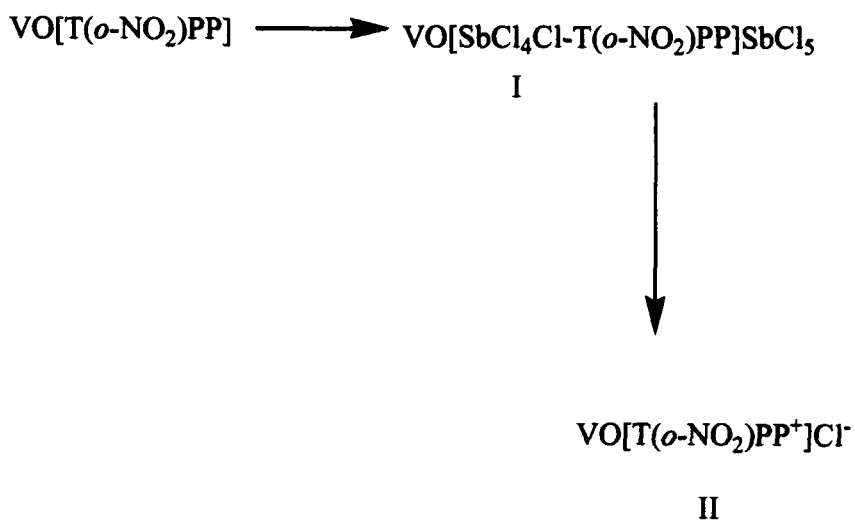
(iv) VO[T(*p*-OH)PP]

Oxidation of VO[T(*p*-OH)PP] with SbCl₅ gives rise to the spectrum(fig.5.7.1(iv)A). Further addition of SbCl₅ give rise to spectrum (fig.5.7.1(iv)B) and the spectrum (fig.5.7.1(iv)C). EPR parameters are summarizing in the table 5.1. The formation of

mono cations is further supplemented by IR spectra¹⁸⁻¹⁹. In all cases an additional band at 1275 cm⁻¹ are observed (fig.5.7.(v)). Further, during the oxidation with SbCl₅, demetallation does not take place. This is checked by taking UV-vis spectra after quenching the solutions containing mono cations and the SbCl₅ with diethyl amine. (fig.5.7.(vi) A, B, C, and D).

5.7.2 DISCUSSION

Except for the VO[T(*p*-OH)PP] other three vanadyl porphyrins undergo oxidation with SbCl₅ in the same manner to that of VOTPP oxidation¹⁴⁻¹⁷. In case of VO[T(*o*-NO₂)PP] It clearly undergoes oxidation quite similar to that of the oxidation of VOTPP. Oxidation steps can be represented as



The pre oxidized form I is observable at room temperature. Further, it forms triplet state (II) on further addition of SbCl₅ and its

spectrum is observable at a higher modulation¹⁶. The EPR parameters are obtained using the simulation program.

In the case of VO[T(*p*-OH)PP] formation of solids(precipitates) on further addition of SbCl₅ is observed. This is due to polymerization which is also observed by some earlier workers²⁰. This is also evident from the CV study. The cations of these vanadyl porphyrins give two g-values indicating that the ligand field possesses an axial symmetry

5.7.3. CONCLUSION

From the EPR study of the oxidation of VO[T(2,5-(OCH₃)₂)PP], VO[T(*p*-OH)PP], VO[T(*o*-NO₂)PP], and VO[TpyP] with SbCl₅ following observations are made

- i) Except VO[T(*p*-OH)PP] all three vanadyl porphyrins undergo oxidation with SbCl₅ generating radical cations in the same process to that of the oxidation of VOTPP.
- ii) The pre-oxidized species are also observable at room temperature. The triplet state spectra are observable at higher modulation even at room temperature.
- iii) The inter-electronic distances ranging between 3.629A° – 3.601A° are observed which points to a_{2u} ground state.
- iv) VO[T(*p*-OH)PP] polymerizes on oxidation.

Table.5.1: ESR spectrum of Vanadyl porphyrins at Room Temperature

Metalloporphyrin	Inter electron distance $R(A^{\circ})$	Unoxidized g value	Oxidized g value		Oxidized A(G) Value	
			g_{\parallel}	g_{\perp}	A_{\parallel}	A_{\perp}
VO[T(2,5-(OCH ₃) ₂)PP]	3.629	1.984	1.932	1.971	2.349	1.768
VO[T(p-OH)PP]	3.621	1.999	1.920	1.989	3.280	1.949
VO[T(o-NO ₂)PP]	3.612	1.975	1.928	1.969	3.620	1.940
VO[TpyP])	3.601	1.987	1.911	1.963	3.009	2.422

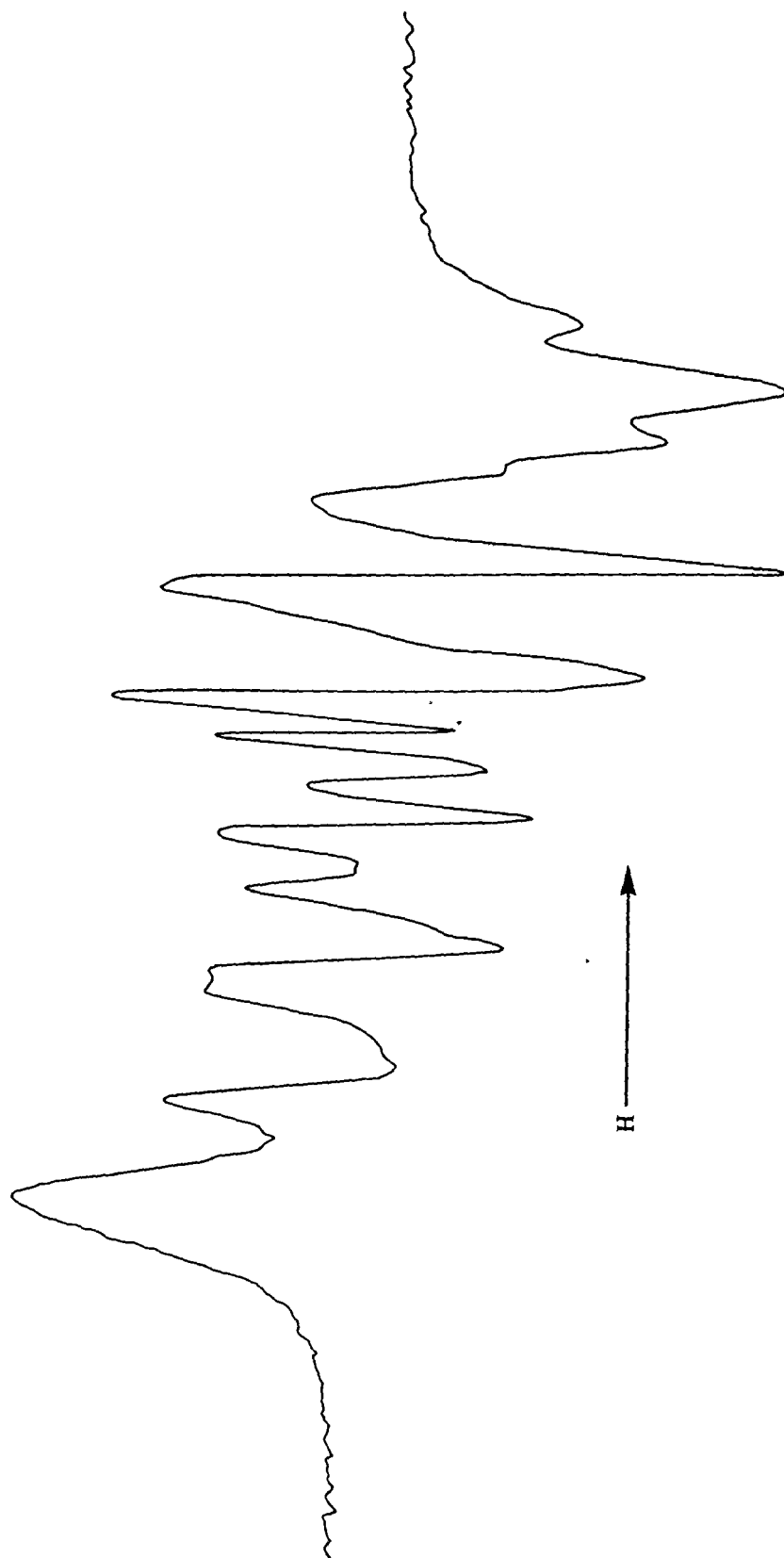


Fig.5.7.1(i). X-band EPR spectra of VO[T(*o*-NO₂ PP)] in CH₂Cl₂ oxidized with SbCl₅ at room temperature

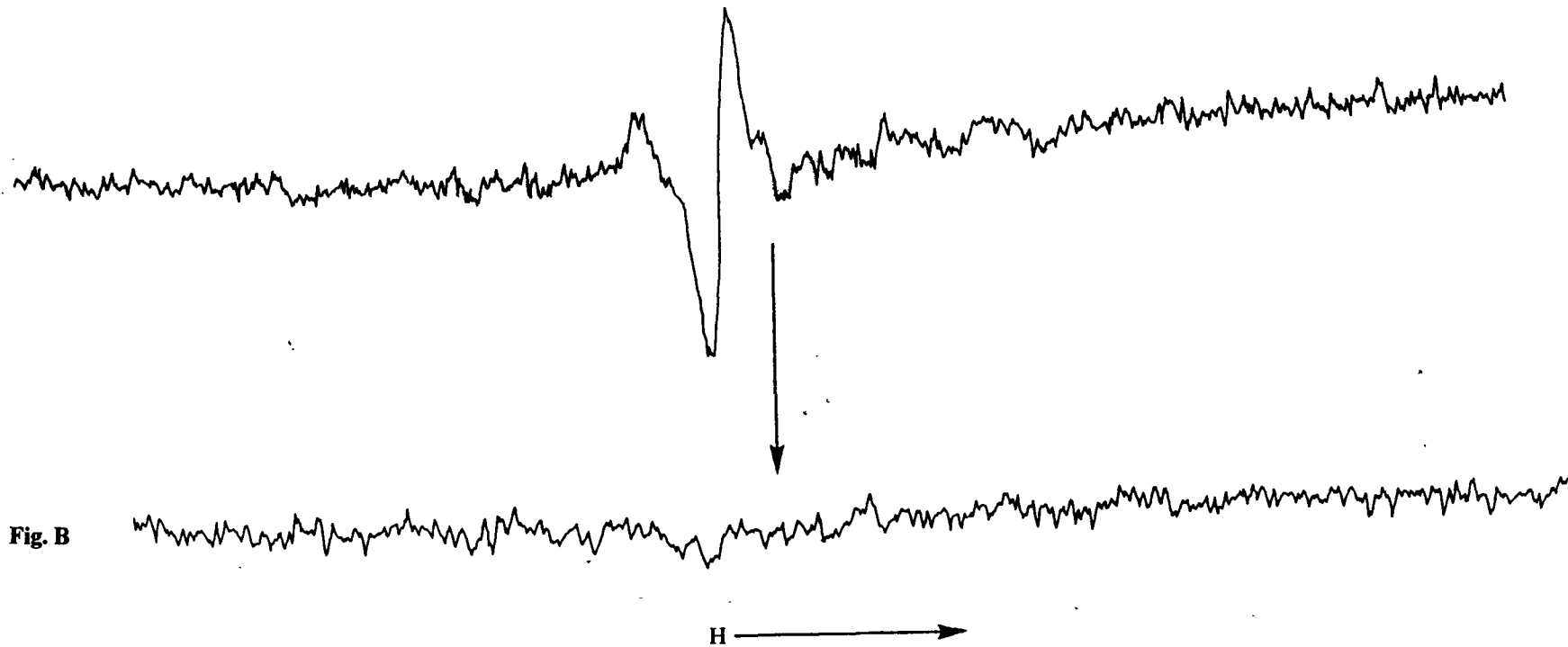


Fig. B

Fig.5.7.1(ii)A and B. X-band EPR spectra of VO[T(2,5-(OCH₃)₂)PP] in CH₂Cl₂ oxidized with SbCl₅ at room temperature.

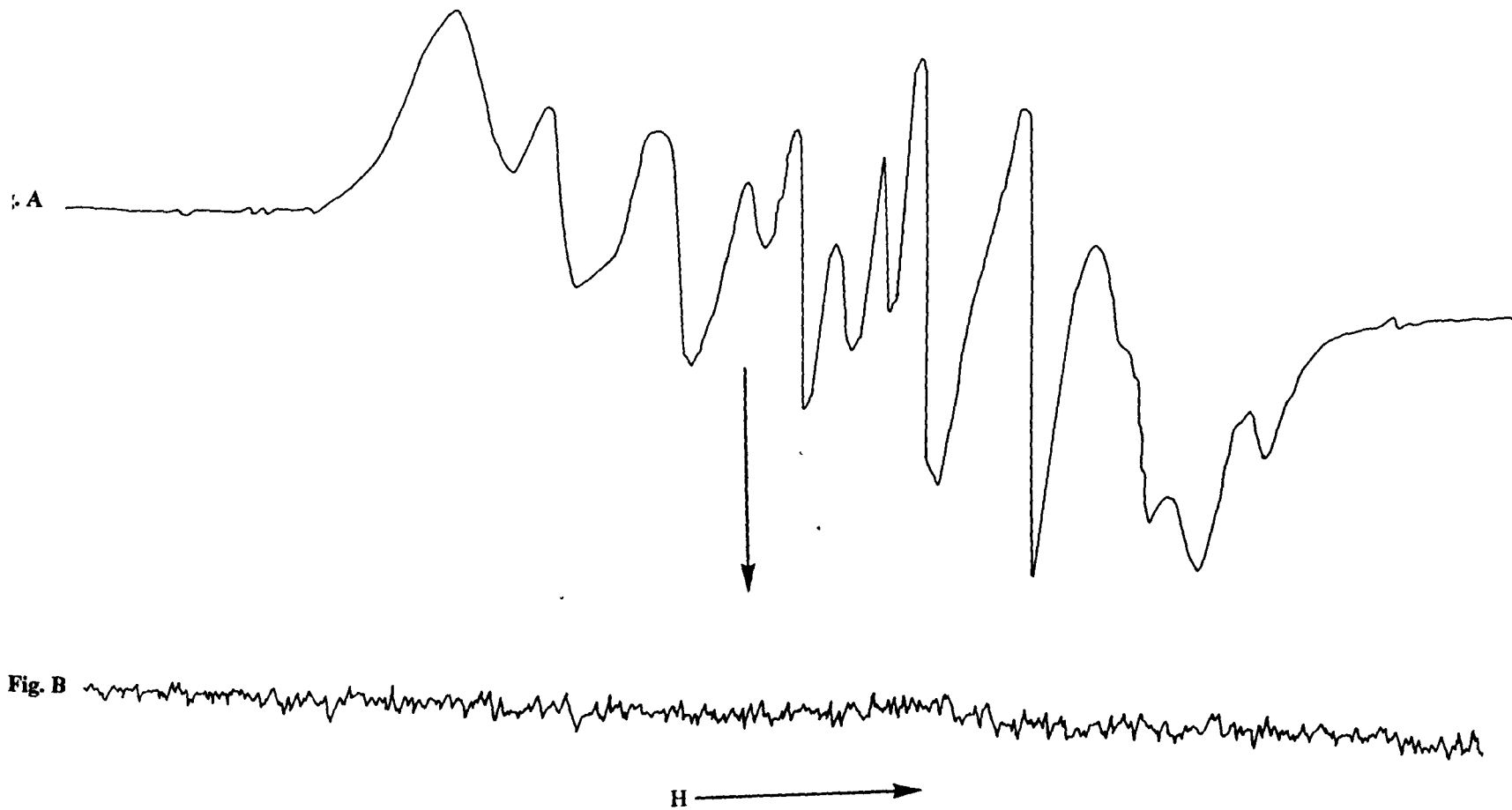


Fig.5.7.1(iii)A and B. X-band EPR spectra of VO[TpyP] in CH₂Cl₂ oxidized with SbCl₅ at room temperature

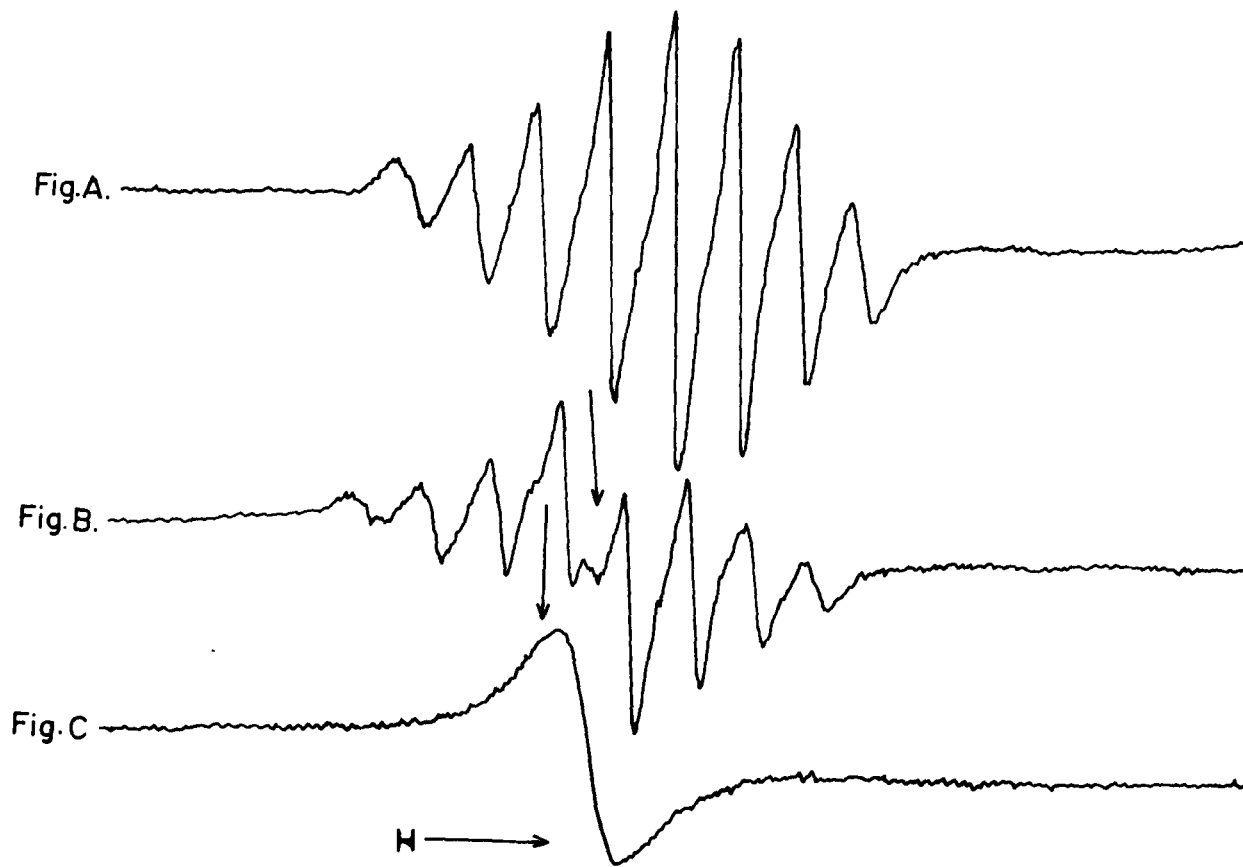


Fig.5.7.1(iv). X-band EPR spectra of VO[T(p-OH)PP] in CH_2Cl_2 .
(A) Unoxidized at room temperature
(B) And **(C)** oxidized with SbCl_5 at room temperature

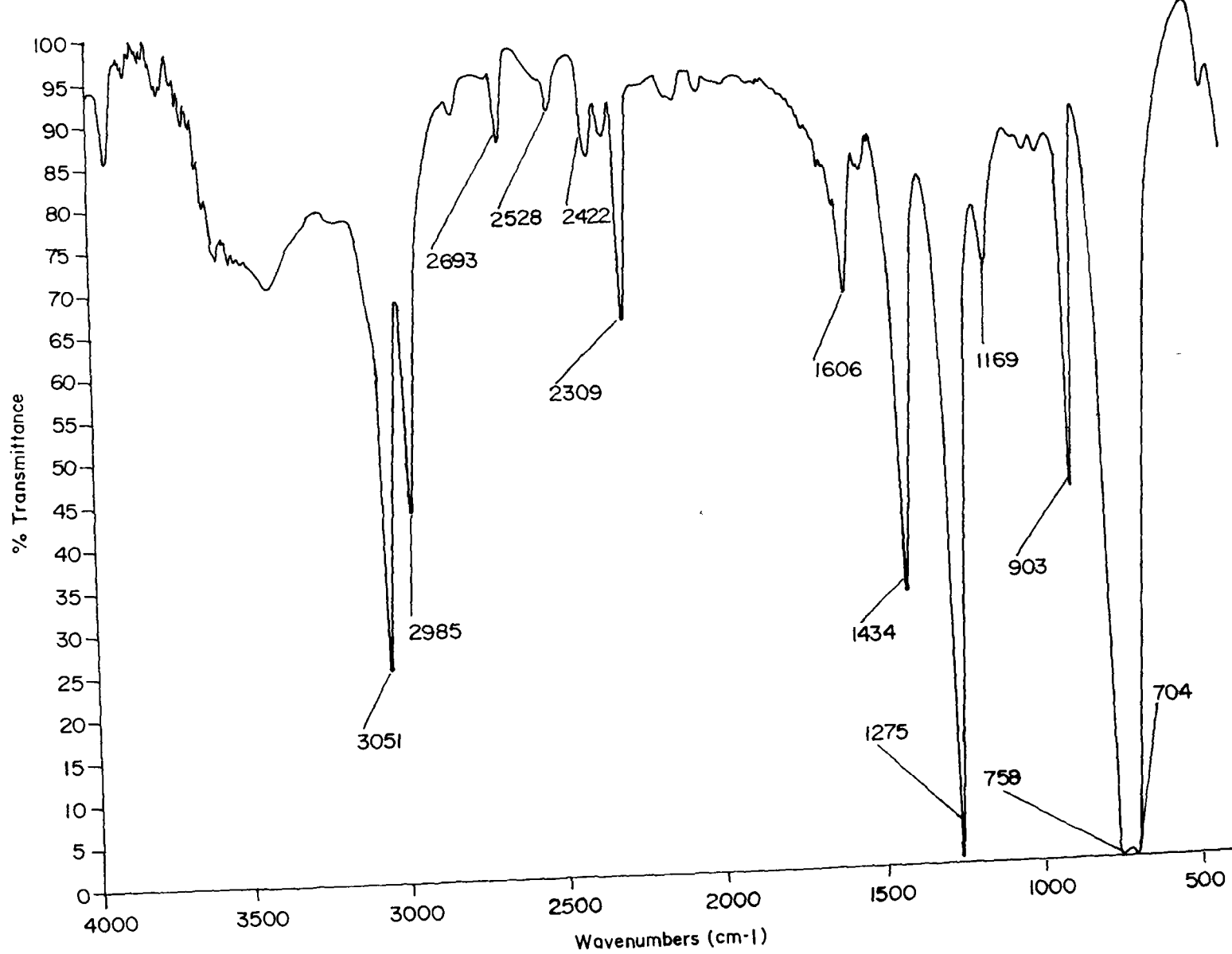


fig.5.7.(v) Infrared spectrum of VO[T(2,5-(OCH₃)₂)PP] in CH₂Cl₂ oxidized with SbCl₅ at room temperature

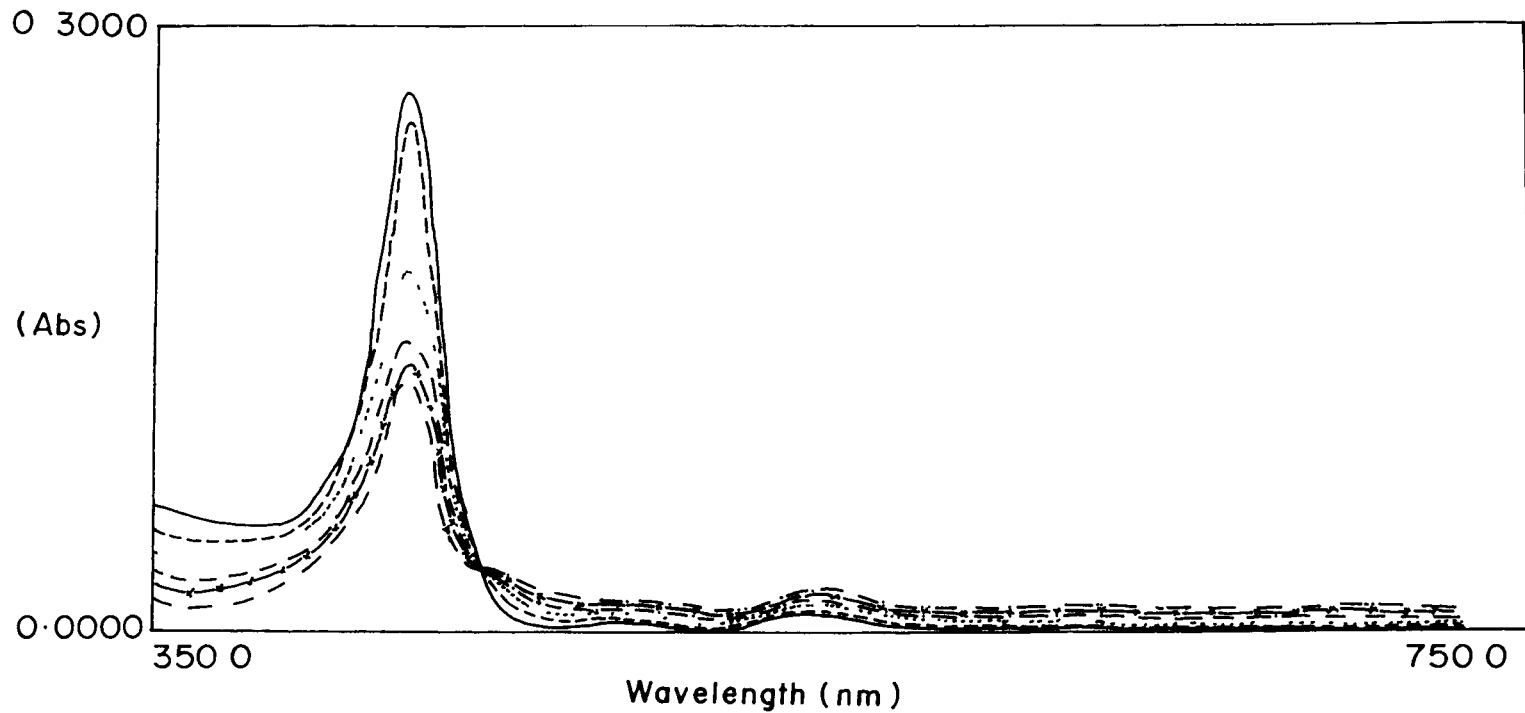


Figure.5.7.1 (vi) A. UV-visible absorption spectrum of VO[T(2,5-(OCH₃)₂)PP] in CH₂Cl₂ oxidized with (____) SbCl₅ at room temperature, (.....), and (----) reduced with diethyl amine

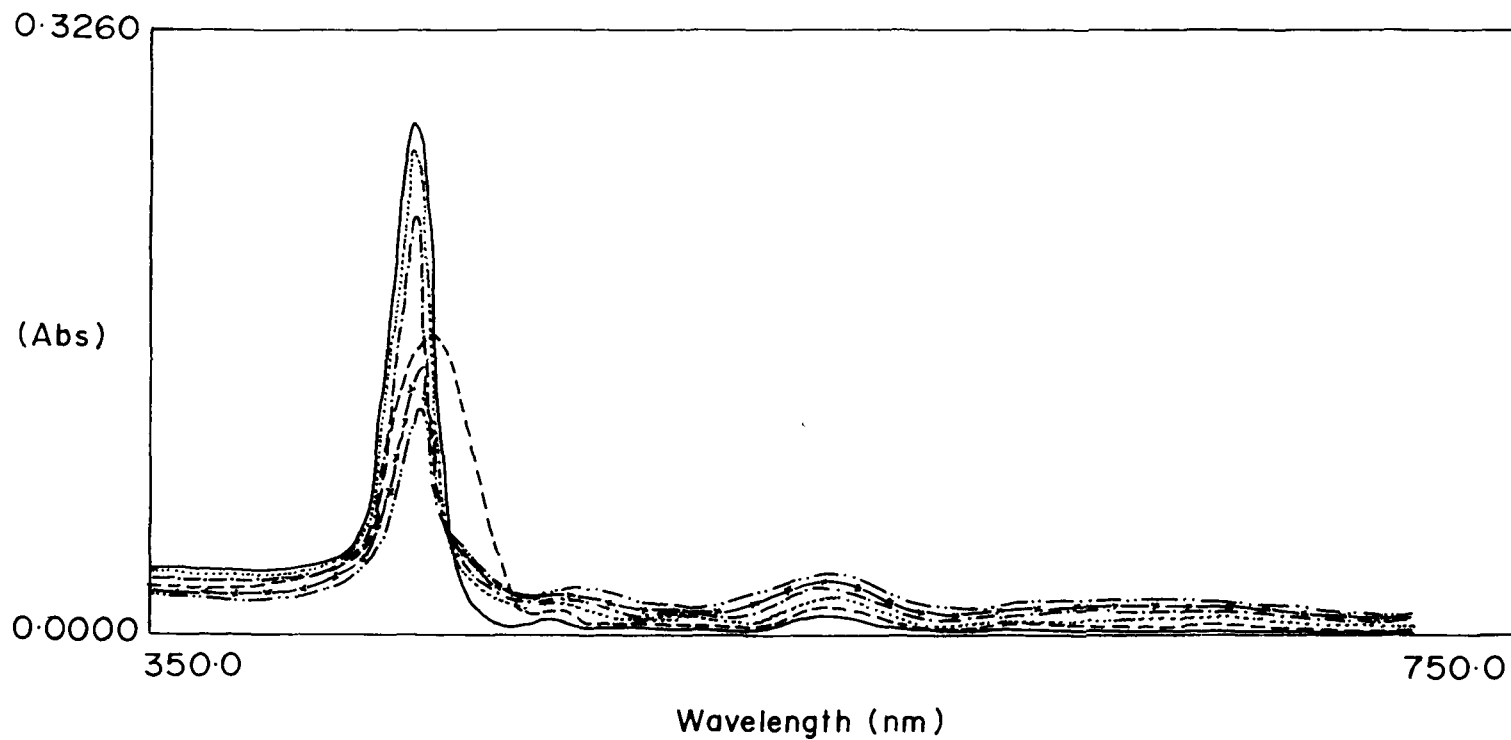


Figure.5.7.1 (vi) B..UV-visible absorption spectrum of VO[T(p-OH)PP]in CH₂Cl₂ oxidized with(____)SbCl₅ at room temperature, (....), ... and (----) reduced with diethyl amine

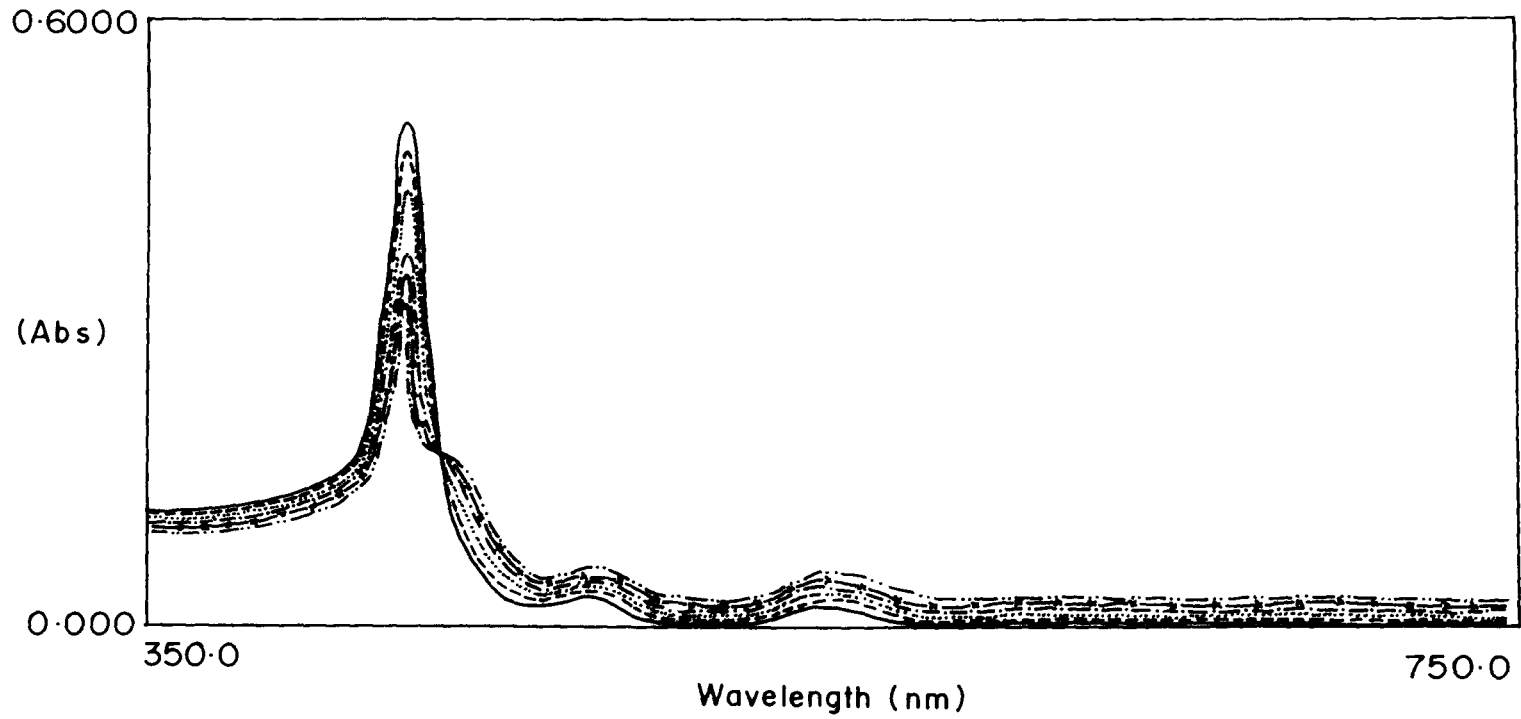


Figure.5.7.1 (vi) C..UV-visible absorption spectrum of VO[T(*o*-NO₂)PP] in CH₂Cl₂ oxidized with(____)SbCl₅ at room temperature, (.....), :..... and (----) reduced with diethyl amine

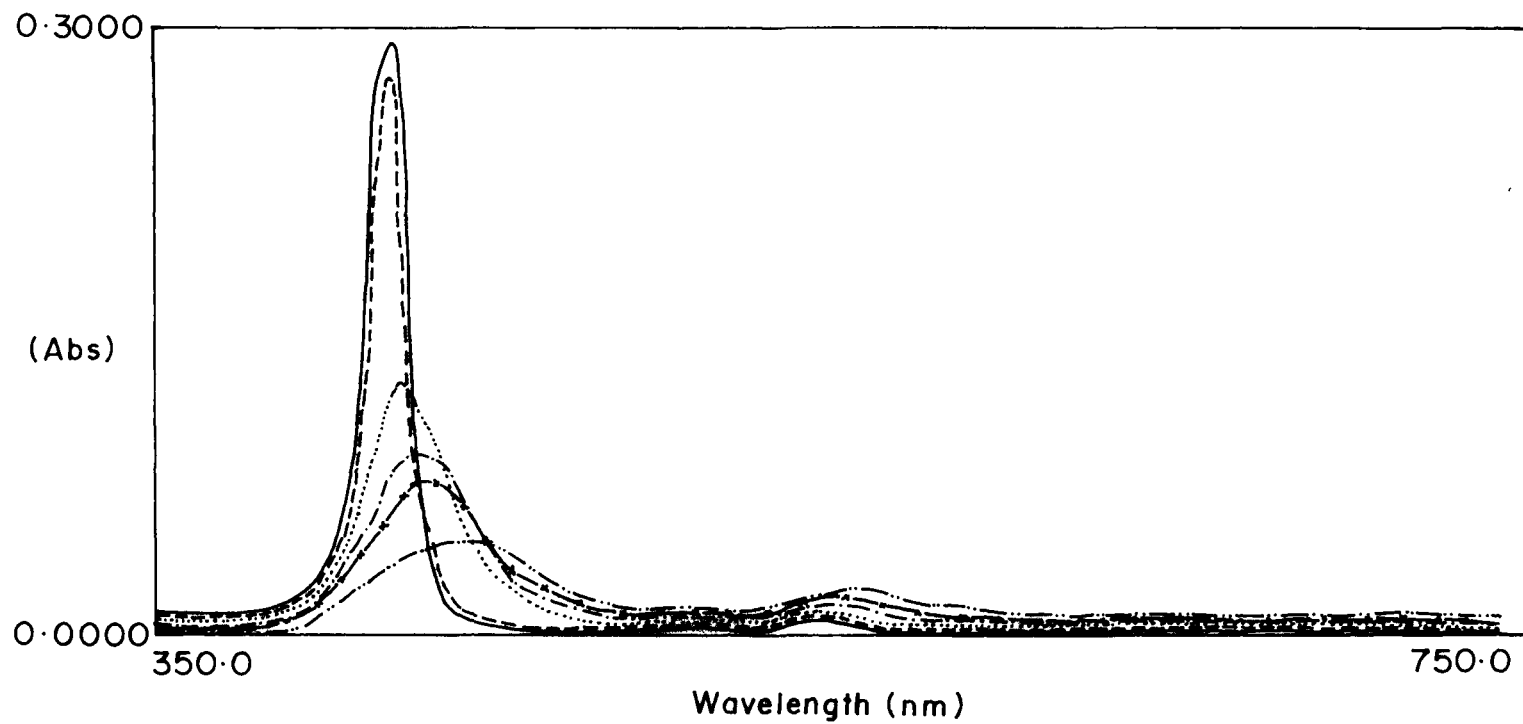


Figure.5.7.1 (vi) D..UV-visible absorption spectrum of VO[TpyP] in CH_2Cl_2 oxidized with(____) SbCl_5 at room temperature, (.....), and (----) reduced with diethyl amine

REFERENCES

1. N. M. Atherton., "*Electron spin Resonance-theory and application*" Ellis Harwood limited, Sussex, England(1973)
and references there in
2. J.E. Wertz and J.R.Bolton, "*Electron spin resonance-Elementary theory and Practical application*" Edition McGraw Hill New York(1972) and references there in
3. A. Carrington and A. D. McLahlen, "*Introduction to Magnetic resonance*" Harper and Row, New York(1967)
and references there in
4. A. Abragan and B. Bleaney, "*Paramagnetic resonance of transition metal ions*" Oxford University press (1970) and
references there in
5. B. R. McGarvey in "*Transition metal chemistry*", Vol.3, R. L. Carlin (Ed.), Marcel Dekker, New York (1966) and
references there in
6. H. M. Schwalz., J. R. Bolton and D. C. Borg(Eds.),"
Biological application of electron spin resonance" Wiley
Inter science, New York (1972) and references there in
7. J. Subramanian, in "*Porphyrins and metalloporphyrins*"
Edited by K. M. Smith (Elsevier, Amsterdam, 1975), p555
and references there in

8. K. M. Smith, in "*Porphyrin and Metalloporphyrins*", Edited by K. M. Smith(Elsevier, Amsterdam, 1975) p3 and references there in
9. J. Fajer, D. C. Borg, A. Forman, D. Dolphin and R. H. Felton., *J. Am. Chem. Soc.*, **92**, 3451 (1970) and references there in
10. J. H. Fuhrhop and D. Mauzerall., *J. Am. Chem. Soc.*, **90**, 3875 (1968) and references there in
11. R. H. Felton, D. Dolphin, D. C. Borg and J. Fajer., *J. Am. Chem. Soc.*, **91**, 196 (1969) and references there in
12. R. H. Felton, in *Porphyrins*, Edited by D. Dolphin (Acad.Press. NY, 1978) **Vol.III**, Chap.1 and references there in
13. M. Gouterman, in *Porphyrins*, Edited by D. Dolphin (Acad.Press. NY, 1978) **Vol.III**, Chap.1 and references there in
14. G. E. Selyutin, A. A. Shklyayev, and V. F. Anerfrienko., *Dokl.Akad.Nauk.SSR.*, **255 (2)**, 390 (1980) and references there in
15. M. Hoshino, S. Konishi, M. Imamura, S. Watanable, and Y. Hana., *Chem. Phys. lett.*, **102**, 259 (1983) and references there in

16. A. Tomba Singh and A. Lemtur, *Spec. Chim. Acta. Part. A* ., **59**, 1549 (2003) and references there in
17. J. Fajer, D. C. Borg, A. Forman, D. Dolphin, R. H. Felton, J. *Am. Chem. Soc* **92**, 3451 (1970) and references there in
18. E. T. Shimomura, M. A. Phillipi, M. M. Goff, W. F. Schuls and C. A. Reed., *J. Am. Chem. Soc.*, **103**, 6778 (1981) and references there in
19. A. S. Hinman, B. J. Pavelick, K. McGarty, *Can. J. Chem.*, **66**, 1589 (1988) and references there in
20. A. Bettelheim, B. A. White, S. A. Raybuck and R. W. Murray., *Inorg .Chem.*, **26**, 1009 (1987) and references there in

NEHU LIBRARY
Acc. No. 104334
Acc. by B. Bamora
Date 17/8/12
Class by. _____
Sub - Heading by. _____
Enter by. _____